

AD-A103 522

OPTICAL COATING LAB INC SANTA ROSA CA F/8 11/3
FABRICATION OF INTEGRAL SOLAR CELL COVERS BY THE PLASMA ACTIVAT--ETC(U)
JAN 81 H S SUREV F33615-79-C-2046

UNCLASSIFIED

AFMNL-TR-80-2124

NL

[OR]
A103522

END
DATE
FILMED
40-81
DTIC

AD A103522

17
AFWAL-TR-80-2124
19



6
**FABRICATION OF INTEGRAL SOLAR CELL
COVERS BY THE PLASMA ACTIVATED SOURCE.**

10
H. S./GUREV

**OPTICAL COATING LABORATORY, INC.
P. O. BOX 1599
SANTA ROSA, CALIFORNIA 95402**

11
JAN 1981

12 77 13 F33615-77-2-2740
TECHNICAL REPORT AFWAL-TR-80-2124

Final Report, ~~January 1979~~ June 1979 to September 1980
21 214-1211

Approved for public release; distribution unlimited.

**AERO PROPULSION LABORATORY
AIR FORCE WRIGHT AERONAUTICAL LABORATORIES
AIR FORCE SYSTEMS COMMAND
WRIGHT-PATTERSON AIR FORCE BASE, OHIO 45433**

DTIC
S 1 1981
D

DTIC FILE COPY


81 9 01 017


NOTICE

When Government drawings, specifications, or other data are used for any purpose other than in connection with a definitely related Government procurement operation, the United States Government thereby incurs no responsibility nor any obligation whatsoever; and the fact that the government may have formulated, furnished, or in any way supplied the said drawings, specifications, or other data, is not to be regarded by implication or otherwise as in any manner licensing the holder or any other person or corporation, or conveying any rights or permission to manufacture use, or sell any patented invention that may in any way be related thereto.

This report has been reviewed by the Office of Public Affairs (ASD/PA) and is releasable to the National Technical Information Service (NTIS). At NTIS, it will be available to the general public, including foreign nations.

This technical report has been reviewed and is approved for publication.


JAMES F. HOLT
Project Engineer


JOSEPH WISE
TAM, Solar/Thermal Power
Energy Conversion Branch

FOR THE COMMANDER


JAMES D. REAMS
Chief, Aerospace Power Division
Aero Propulsion Laboratory

"If your address has changed, if you wish to be removed from our mailing list, or if the addressee is no longer employed by your organization please notify AFWAL/POOC-2, W-PAFB, OH 45433 to help us maintain a current mailing list".

Copies of this report should not be returned unless return is required by security considerations, contractual obligations, or notice on a specific document.

REPORT DOCUMENTATION PAGE		READ INSTRUCTIONS BEFORE COMPLETING FORM
1. REPORT NUMBER AFWAL-TR-80-2124	2. GOVT ACCESSION NO. 463870 <i>AD-A103522</i>	3. RECIPIENT'S CATALOG NUMBER
4. TITLE (and Subtitle) Fabrication of Integral Solar Cell Covers by the Plasma Activated Source		5. TYPE OF REPORT & PERIOD COVERED June, 1979 - Sept. 1980 Final
7. AUTHOR(s) H. S. Gurev		6. PERFORMING ORG. REPORT NUMBER
9. PERFORMING ORGANIZATION NAME AND ADDRESS Optical Coating Laboratory, Inc. P.O. Box 1599 Santa Rosa, CA 95402		8. CONTRACT OR GRANT NUMBER(s) F33615-79-C-2046
11. CONTROLLING OFFICE NAME AND ADDRESS Aero Propulsion Laboratory (AFWAL/POOC) AF Wright Aeronautical Laboratories, AFSC Wright-Patterson Air Force Base, Ohio 45433		10. PROGRAM ELEMENT, PROJECT, TASK AREA & WORK UNIT NUMBERS 61101F 3145 19 72 62203F
14. MONITORING AGENCY NAME & ADDRESS (if different from Controlling Office)		12. REPORT DATE January 1981
		13. NUMBER OF PAGES 69
		15. SECURITY CLASS. (of this report) UNCLASSIFIED
		15a. DECLASSIFICATION/DOWNGRADING SCHEDULE
16. DISTRIBUTION STATEMENT (of this Report) Approved for public release- Distribution Unlimited		
17. DISTRIBUTION STATEMENT (of the abstract entered in Block 20, if different from Report)		
18. SUPPLEMENTARY NOTES		
19. KEY WORDS (Continue on reverse side if necessary and identify by block number) Solar Cell Cover Plasma Deposition		
20. ABSTRACT (Continue on reverse side if necessary and identify by block number) An RF plasma in oxygen was used as a source for activated oxygen molecules which were reacted with, for example, silane at a solar cell surface to deposit amorphous silicon dioxide on the solar cell, to act as a protective cover. One hundred micrometers of SiO ₂ could be deposited. The coatings exhibited considerable intrinsic stress on 12-mil cells. Attempts to reduce the stress by mixing Al ₂ O ₃ with SiO ₂ were not successful because of insufficient control of the mixing ratio.		

BLACK PAGE

TABLE OF CONTENTS

	<u>Page No.</u>
1.0 INTRODUCTION.....	1
1.1 Integral Solar Cell Covers.....	1
1.2 Requirements for Integral Solar Cell Covers.....	2
1.3 Alternative Approaches.....	3
1.3.1 CVD.....	3
1.3.2 Electron Beam Evaporation.....	3
1.3.3 RF Sputtering.....	3
1.3.4 Ion Beam Sputtering.....	3
1.3.5 Heat Curable Si-O Resins.....	3
1.3.6 Fritted Glasses.....	4
1.3.7 Electrostatic Bonding.....	4
1.3.8 Organic Integral Covers.....	4
1.4 Stress Problem.....	5
1.5 OCLI Plasma Activated Source Evaporation --Prior Experience.....	10
1.6 PAS-CVD.....	12
2.0 EXPERIMENTAL APPROACH.....	19
3.0 EXPERIMENTAL PROCEDURE.....	20
4.0 RESULTS.....	24
4.1 Deposition of SiO ₂ Films.....	24
4.2 Deposition of Al ₂ O ₃ from AlCl ₃	39
4.3 Deposition of Al ₂ O ₃ from Triethylaluminum	43
4.4 Deposition of Mixed SiO ₂ -Al ₂ O ₃ Films.....	46
4.5 SiO ₂ Coatings on Silicon Solar Cells.....	51
4.6 SiO ₂ Coatings in GaAs Solar Cells.....	58
5.0 CONCLUSIONS.....	61
5.1.....	61
5.2.....	61
5.3.....	61
5.4.....	61
5.5.....	62

TABLE OF CONTENTS (continued)

	<u>Page No.</u>
APPENDIX A.....	63
REFERENCES.....	69

Accession For	
NTIS GRA&I	<input checked="" type="checkbox"/>
DTIC TAB	<input type="checkbox"/>
Unannounced	<input type="checkbox"/>
Justification	
By _____	
Distribution/	
Availability Codes	
Dist	Avail and/or Special
A	

DTIC
ELECTE
SEP 1 1981
D

LIST OF ILLUSTRATIONS

<u>Fig. No.</u>		<u>Page No.</u>
1	Average Intrinsic Deposition Stress of Pyrolytic Silicon Oxynitride Films vs. Composition.....	7
2	Coefficient of Linear Expansion of Al_2O_3 - SiO_2 Mixtures.....	8
3	Stresses in $\text{AlN-Si}_3\text{N}_4$ Mixtures.....	9
4	Schematic View of Plasma Activated Source.	11
5	Schematic View of Plasma Activated Source in CVD Mode.....	13
6	Deposition of $\text{SiO}_2 + \text{Al}_2\text{O}_3$ by Evaporation of Solid SiO_2 and In-Cavity Oxidation of an Al Compound.....	16
7	Deposition of $\text{SiO}_2 + \text{Al}_2\text{O}_3$ by In-Cavity Oxidation of a Si Compound and an Al Compound.....	17
8	Deposition of $\text{SiO}_2 + \text{Al}_2\text{O}_3$ by External Oxidation of a Si Compound and an Al Compound in a Plasma Activated Oxygen Discharge.....	18
9	PAS Equipment Installed at OCLI.....	21
10	PAS Activator and Reactant Gas Nozzle.....	22
11	Transmission of Sample 1311-088, Fused Silica Coated with 23.5 μm of SiO_2	25
12	Transmission of Sample 1311-085, Fused Silica Coated with 9.6 μm of SiO_2	26
13	Transmission of Sample 1311-049, Fused Silica Coated with 3.5 μm of SiO_2	27
14	SiO_2 Coating Rate as Measured by Quartz Frequency Monitor during Run 1311-088.....	28
15	Deposition Rate versus RF Power.....	30
16	Deposition Rate versus Gas Ratio.....	31
17	Deposition Rate versus Silane Flow Rate...	32
18	Deposition Rate versus Oxygen Flow Rate...	33
19	SiO_2 Deposition Apparatus Schematic.....	35
20	Deposition Rate versus Silane Delivery Tube Height.....	36
21	Thickness Distribution.....	38
22	Vapor Pressure of AlCl_3	41

LIST OF ILLUSTRATIONS (continued)

<u>Fig. No.</u>		<u>Page No.</u>
23	Transmission of Sample 1311-050, Fused Silica Coated with 2.5 μm of Al_2O_3 by the AlCl_3 Route.....	42
24	Crazing of Al_2O_3 Films on Silicon Substrates.....	45
25	Apparatus for Depositing Al_2O_3 - SiO_2 Mixtures by TEA-Silane Route.....	47
26	Crazing of Al_2O_3 - SiO_2 Films on Silicon Substrates.....	49
27	Transmission of Sample 1311-095, Fused Silica Coated with Al_2O_3 Mixed Oxide (5 μm Thick).....	50
28	Fracture of Silicon Solar Cells after PAS Coating.....	53
29	Residual Stress of Coated Silicon Solar Cells.....	54
A-1	Spectral Distribution of the Simulator Xenon and Tungsten Lamps (Separate and Combined) Compared to Sunlight in Space (Johnson).....	69

LIST OF TABLES

<u>Table No.</u>		<u>Page No.</u>
1	Thermal Expansion Coefficients of Materials.....	6
2	Comparison of Several Coating Methods to Produce SiO_2 by SiH_4 Oxidation.....	14
3	Gas Requirements for PAS-CVD Coating.....	43
4	Electrical Output of PAS Coated Silicon Solar Cells (High Efficiency Violet Cells)	56
5	Electrical Output of PAS Coated Textured Silicon Solar Cells (No AR on Cells).....	57
6	Performance of Coated GaAs Cells.....	58
7	Thermal Shock Resistance of GaAs Cells....	60

BLANK PAGE

1.0 INTRODUCTION

1.1 Integral Solar Cell Covers. Recent trends in space power systems indicate a continuing need for lightweight solar cell arrays. As requirements for power per satellite increase, there will be a desire for lighter weight arrays. State-of-the-art technology currently exists for the manufacture of thin (2 mil) solar cells having high performance, and this program was initiated to develop a lightweight cover with proven performance to protect that cell. Unless new technology can be developed, future space programs may be faced with the prospect of cementing a 4 mil to 12 mil thick cover to a 2 mil cell in order to provide the required cell lifetimes. In addition to this weight penalty, problems can arise at the cover/cell bond as a result of hostile threats to the spacecraft.

Integral solar cell covers offer an improvement in the cell/cover system. They consist of a thick (up to 100 μ m) layer of a suitable dielectric material deposited directly on the surface of the solar cell. None of the processes previously applied to this problem over the past 20 years, offers a cost-effective manufacturing solution.

1.2 Requirements for Integral Solar Cell Covers. Potential performance improvements have fostered extensive R&D efforts to develop useful integral solar cell covers. Their required characteristics include:

1. Low residual stress level after deposition to minimize cell deformation and breakage;
2. Close matching of thermal expansion coefficient to that of the cell to control thermally induced stresses;
3. Strong adhesion to the solar cell surface to avoid delamination caused by either deposition stresses or thermal stresses;
4. High optical transmission in the spectral range (400-1100 nm) of cell operation to maximize cell performance;
5. Improved emittance over bare solar cells to control operating temperatures;
6. Resistance to darkening caused by radiation levels associated with specific satellite missions to ensure adequate power system lifetime;
7. Ease of deposition at a practical rate for low production costs; and
8. Provide a suitable surface for optical coatings to satisfy additional requirements.

1.3 Alternative Approaches. A variety of coating approaches have been proposed and investigated in the past, primarily for silicon cells. Thus far, none appears to meet the required criteria.

1.3.1 CVD. Chemical vapor deposition from silane-type compounds at substrate temperatures in the range 400-900°C led to severe cell degradation and relatively poor film quality when thickness exceeded 1 μ m.¹

1.3.2 Electron Beam Evaporation. Deposition of aluminosilicate glass at rates in excess of 0.6 μ m/min. has been reported.² The films have severe darkening due to suboxide formation, and very high stress levels. Effort to avoid the suboxides by reactive evaporation in oxygen leads to oxidation failures in the cell contact metallization since the substrate temperature was in excess of 300°C.

1.3.3 RF Sputtering. Though this technique limits solar cell heating to less than 200°C, deposition rates are about an order of magnitude slower than electron beam evaporation. Hence projected process economics are not considered promising although cell cover properties are attractive.³

1.3.4 Ion Beam Sputtering. Film properties appear promising, but the process is inherently even slower than RF sputtering.⁴

1.3.5 Heat Curable Si-O Resins. Preliminary results on cured silicone resins indicate that losses in the short-circuit current after UV irradiation of the cells is a significant problem.⁵

1.3.6 Fritted Glasses. Special low fusion temperature glass powders permit cover fabrication at 520°C. Though the process is simple, rapid, and economically attractive, the solar cells are thermally degraded during processing.⁶

1.3.7 Electrostatic Bonding. The feasibility of a practical, inexpensive production process has yet to be reported.

1.3.8 Organic Integral Covers. Adequate radiation resistance to the environment in space has not yet been demonstrated for these materials.

1.4 Stress Problem. The stress state of a coated substrate can be divided into two distinct categories:

- a. Intrinsic deposition stresses. If a substrate is coated at an elevated temperature and evaluated at room temperature, its stress state will include the effects of accommodation of the dissimilar coating substrate structures during the coating process, stress relaxation after coating and the thermal stresses induced by cooling to room temperature. The magnitude and direction of these intrinsic stresses generally depend on process conditions in a reproducible manner but are difficult to predict from basic material properties of the coating and substrate.
- b. Thermal stresses. On the other hand, stresses induced by subsequent thermal excursions can be readily predicted from knowledge of the differential in thermal expansion coefficients, elastic constants, geometry, etc.

Table 1 presents the thermal expansion coefficients of several materials of interest in the Al-Si-N-O quaternary system. The large thermal mismatch between Si and SiO_2 is readily apparent. Since this is a material property of these substances, differential thermal stresses will be encountered whenever the combination is heated or cooled.

Table 1
Thermal Expansion Coefficients of Materials

<u>Material</u>	<u>Coeff. of Thermal Exp.</u> ppm/°C
Si	4.2
GaAs	5.8
SiO ₂ (fused silica)	0.5
Al ₂ O ₃	8.0
Si ₃ N ₄	2.69
AlN	4.89

Previous workers have shown that mixed films which have excellent thermal expansion matching to Si can be deposited in this quaternary system by a variety of methods. Some of these low thermal stress films include SiO₂ + Si₃N₄ (Fig. 1)⁷; AlN + Si₃N₄ (Fig. 2)⁸; and Al₂O₃ + SiO₂ (Fig. 3)⁹. (For convenience, the mixed films are designated by their binary components. This does not imply that they are simple two phase mixtures. Indeed, most of these mixed films have been shown to have an amorphous structure.)

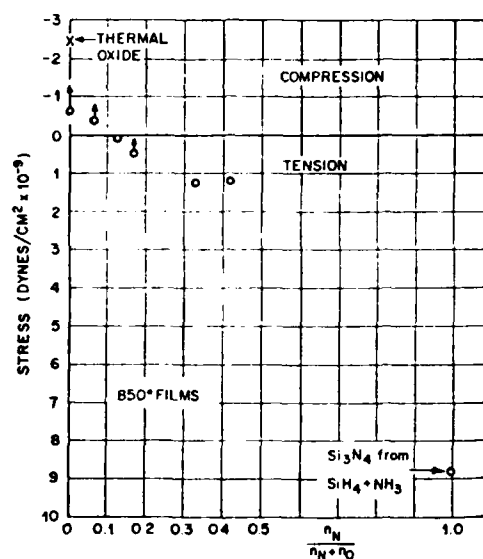


Figure 1
Average Intrinsic Deposition Stress Of
Pyrolytic Silicon Oxynitride Films vs. Composition⁷

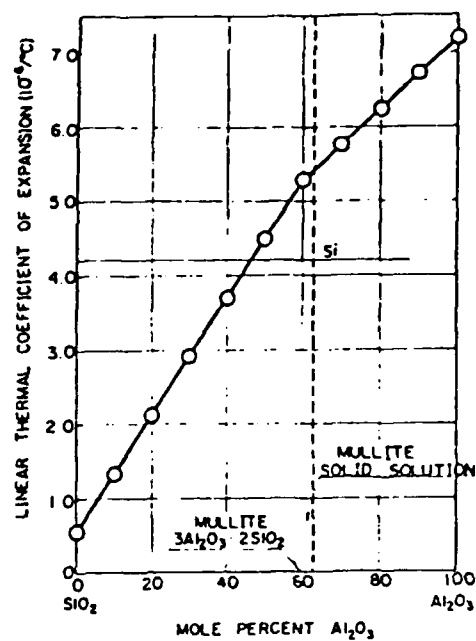


Figure 2
Coefficient of Linear Expansion of
 Al_2O_3 - SiO_2 Mixtures⁸

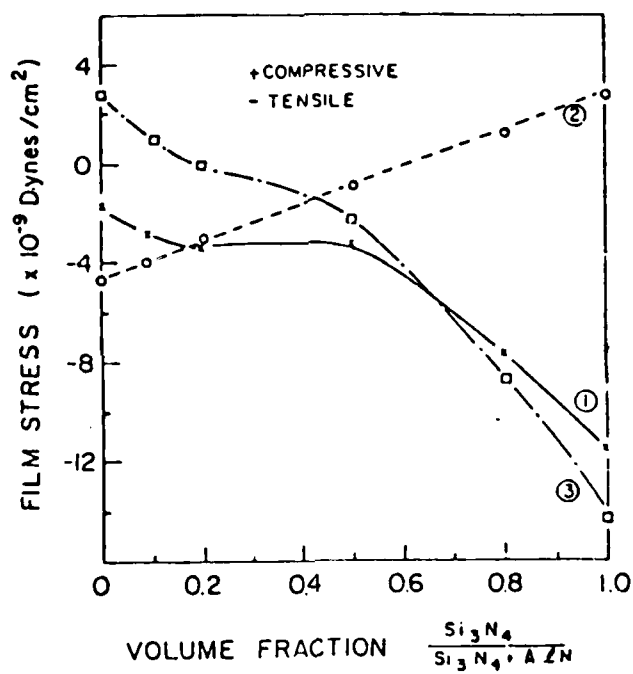


Figure 3
Stresses in AlN-Si₃N₄ Mixtures⁹

1.5 OCLI Plasma Activated Source Evaporation--

Prior Experience. As originally employed by Optical Coating Laboratory, Inc., (OCLI), the Plasma Activated Source (PAS) is basically a reactive evaporation tool which employs an oxygen plasma both as the heat source to evaporate the coating material and as the activation agent which promotes full oxidation of the deposited oxides (Fig. 4). The plasma is generated within a cylindrical source and the activated source vapor escapes from a small hole in one end. With proper thermal shielding, radiation loss is confined to the exposed aperture area, which is significantly smaller than the area of cylindrical face being evaporated. Because of this areal constraint, radiation heating of substrates is markedly reduced. PAS-evaporation is a batch coating process. Evaporation rate varies during a run as the source consumes itself and the process ceases when the source loses its shape.

Employing the PAS as an evaporation source (Fig. 4), we could deposit SiO_2 layers as thick as 30-35 μm at rates as high as 5-6 $\mu\text{m}/\text{min}$. The deposition of fully oxidized SiO_2 , however, was limited to 1-2 $\mu\text{m}/\text{min}$. because the existing pumping system limited oxygen flow to the plasma.

Preliminary tests were performed on silicon solar cells covered with PAS-deposited SiO_2 layers as thick as 20 μm . Since these films were not deposited at a high enough O_2/SiO_2 ratio to suppress suboxide formation, their absorptance produced moderate degradation in cell power output. When the coating was removed, the bare solar cell exhibited no measurable degradation from the coating process. Good coating adhesion was noted.

As would be expected in any SiO_2 system, the main problem encountered with PAS-evaporated SiO_2 coatings on solar cells was the severe compressive stresses encountered in the films and the resultant warpage and breakage of cells.

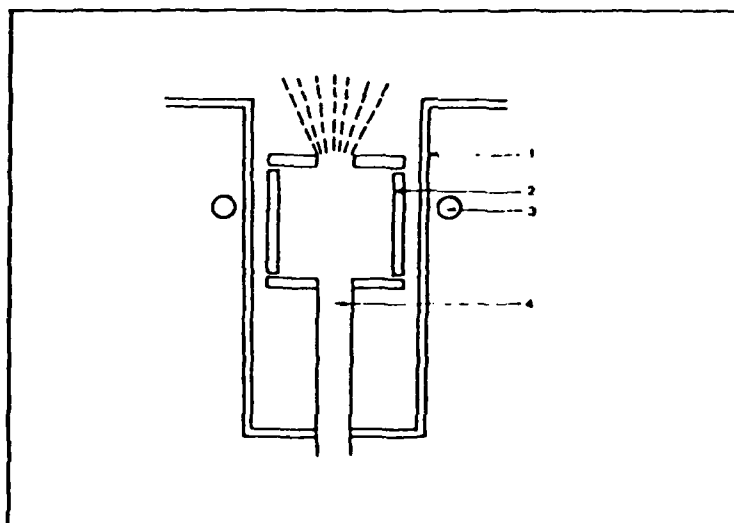


Figure 4
Schematic View of Plasma Activated Source

- 1) Quartz Vacuum Chamber
- 2) Cavity Constructed of Material to Be Deposited
- 3) RF Induction Coil
- 4) Gas Supply Tube

1.6 PAS-CVD. Prior to the initiation of the current program, we developed several novel coating processes which employ the PAS source in modified forms. One mode of operation showed promise for the continuous deposition of thick oxide films and became the subject of this study. As indicated in Fig. 5, oxygen is activated in the PAS source which is run at a power sufficiently low to avoid evaporation of its walls. Hence, this is a continuous, steady state coating process, unlike its parent, PAS-evaporation.

The desired oxide films are deposited by chemical reaction between the activated oxygen and the reactant vapor introduced into the plasma region. (As shown later, nitride films can also be formed using a nitrogen plasma.)

It would be useful to compare this new process with several others which are similar in several respects (Table 2) and which can also be used to deposit SiO_2 by silane oxidation.

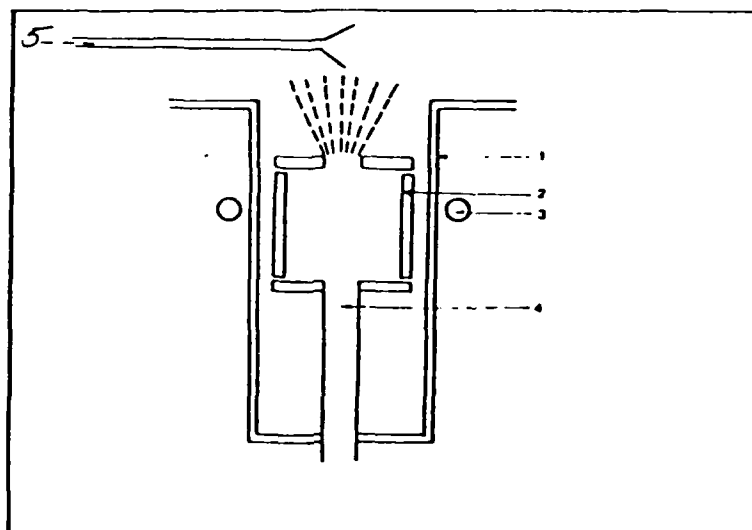


Figure 5
Schematic View of Plasma Activated Source in CVD Mode

- 1) Quartz Vacuum Chamber
- 2) Fused Quartz Cavity
- 3) RF Induction Coil
- 4) Oxygen Supply Tube
- 5) Reactant Gas Supply Tube

Table 2
Comparison of Several Coating Methods
To Produce SiO_2 by SiH_4 Oxidation

<u>PROCESS</u>	<u>PRESSURE</u>	<u>TEMPERATURE</u>	<u>ACTIVATION</u>
Plasma CVD	10^{-1} - 1 torr	100 - 250°C	Capacitively Coupled
Low Pressure CVD	10^{-1} - 1 torr	350 - 500°C	None
PAS	10^{-4} - 10^{-3} torr	50 - 150°C	Inductively Coupled with PAS activator

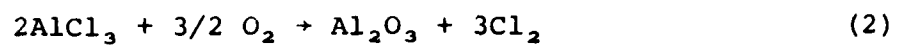
To obtain the desired film composition, one or more of the constituents is introduced to the system as a compound vapor and chemically reacted to the required oxide (or nitride) either within the source or at the solar cell surface. For example, SiO_2 + Al_2O_3 films could be deposited by several methods.

The SiO_2 component could be formed by either:

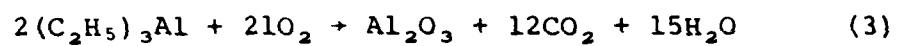
- a. Evaporation of the solid SiO_2 source cavity,
- b. Oxidation of a silicon-bearing gaseous compound such as silane by the reaction:



On the other hand, the low vapor pressure of Al_2O_3 makes evaporation of a solid source an unattractive process. Hence, the Al_2O_3 would be deposited by oxidation of a gaseous source such as AlCl_3 or an alkyl (e.g., triethyl aluminum, $(\text{C}_2\text{H}_5)_3\text{Al}$) by the reactions:



or,



Several of the combinations of Si_2 and Al_2O_3 sources which can be employed are illustrated in Figs. 6 to 8.

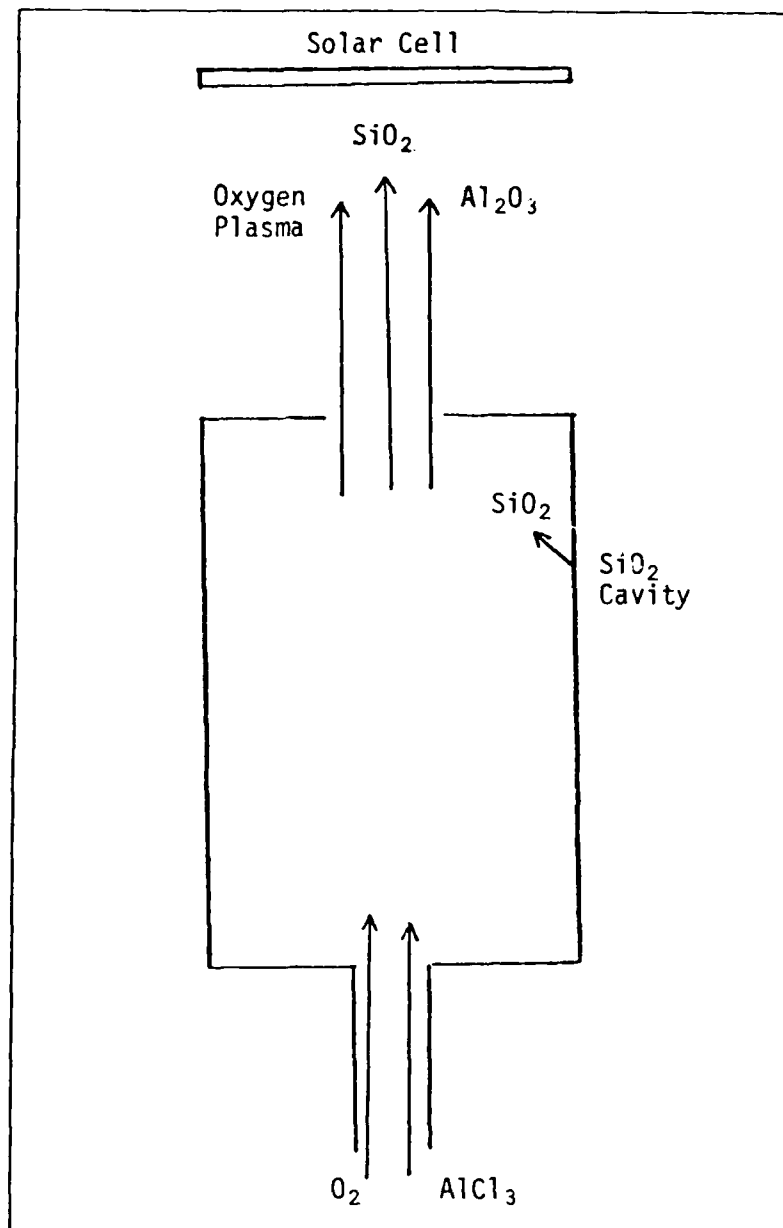


Figure 6
Deposition of $\text{SiO}_2 + \text{Al}_2\text{O}_3$ by Evaporation of Solid
 SiO_2 and In-Cavity Oxidation of an Al Compound

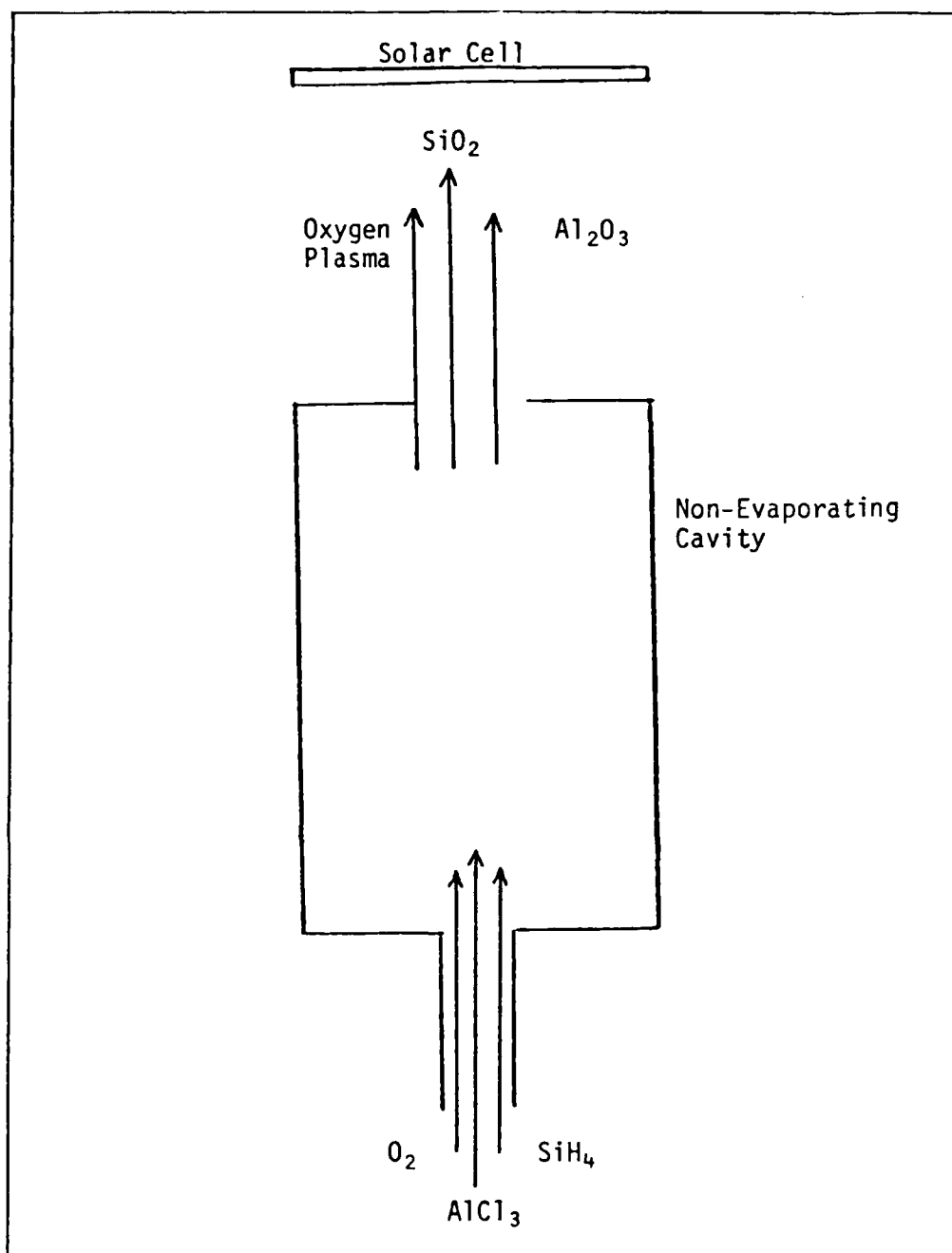


Figure 7
Deposition of $\text{SiO}_2 + \text{Al}_2\text{O}_3$ by In-Cavity
Oxidation of a Si Compound and an Al Compound

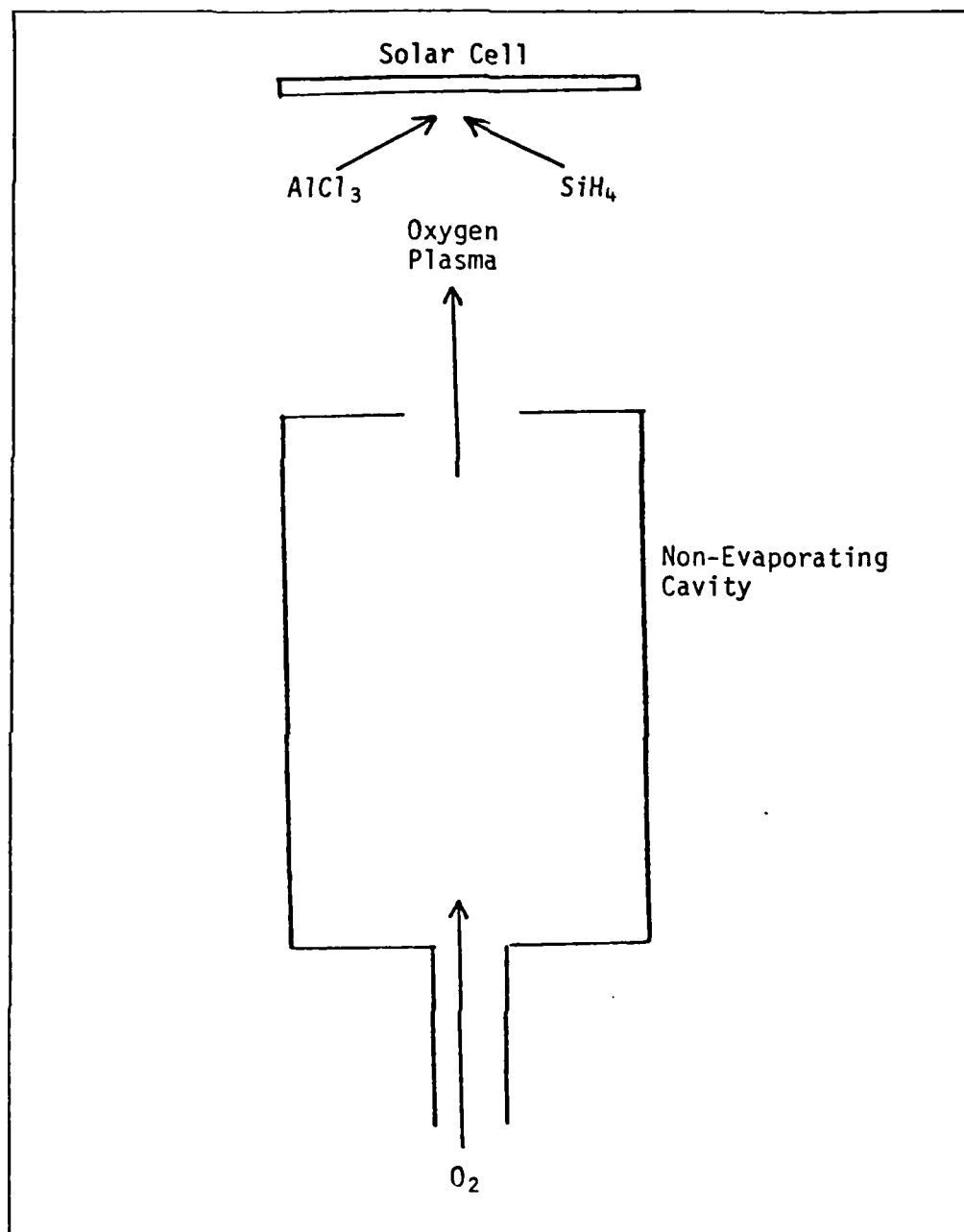


Figure 8
Deposition of $\text{SiO}_2 + \text{Al}_2\text{O}_3$ by External
Oxidation of a Si Compound and an Al
Compound in a Plasma Activated Oxygen Discharge

2.0 EXPERIMENTAL APPROACH

The current program was undertaken to demonstrate the feasibility of depositing thick coatings as integral solar cell covers by the PAS-CVD process, and measuring the resultant cell properties. The tasks performed included:

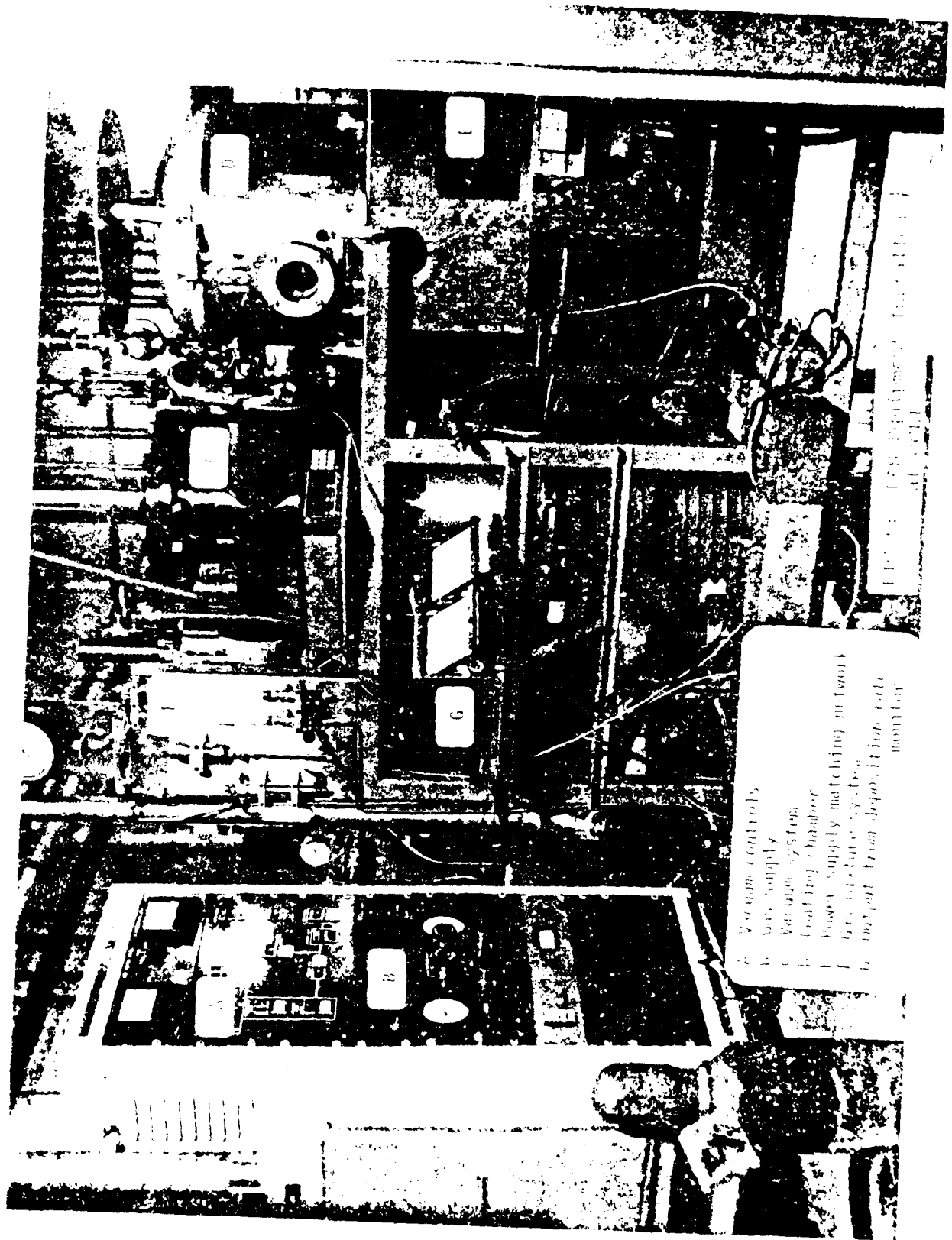
1. Demonstrate the feasibility of depositing on silicon wafer substrates coatings of a pure film of SiO_2 , Al_2O_3 and Si_3N_4 . Deposit mixtures of these dielectrics: $\text{SiO}_2 - \text{Al}_2\text{O}_3$ and $\text{SiO}_2 - \text{Si}_3\text{N}_4$.
2. Deposit integral covers, from 25 to 100 μm thick, onto Si and GaAs solar cells.
3. Determine the electrical and mechanical behavior of the coated cells.

3.0 EXPERIMENTAL PROCEDURE

The coating apparatus employed for these studies is pictured in Figures 9 and 10. An oxygen or nitrogen plasma is generated by inductively coupling an RF field (13.56 MHz) to the gas flowing through a small (49 mm dia. x 50 mm long) fused silica tube. The plasma escapes from the activation source through an exit hole in the tube and fills the vacuum chamber. While the coating chamber has vacuum in the 10^{-4} to 10^{-3} torr range, the pressure in the activation source must be substantially higher to sustain the plasma discharge. Although tube pressure has not been directly measured in the plasma, measurements made with inert gases at the same flow rate indicate that tube pressure is near 1 torr which is consistent with the pressure required to sustain an oxygen plasma.

The reactant gas is introduced through a perforated nozzle ring mounted parallel to the substrate midway between substrate and activator tube. The activator substrate spacing could be varied over the range from 5 cm to 25 cm and was typically 20 cm.

The substrates were mounted on an aluminum holder. They were heated only by radiation from the activator and their temperature, as measured by thermocouples imbedded in the holder, depended on the power level used to induce the plasma. The maximum substrate temperature did not exceed 150°C even for extended runs at high power.



Vacuum controls
Gas supply
Vacuum system
Leakage chamber
Gas supply matching network
Temperature system
Input from deposition rate
monitor



Figure 10
PAS Activator and Reactant Gas Nozzle

Coatings were evaluated by a variety of techniques which included:

1. Thickness measurement by surface profilometer employing the Dektak, model 900050, by Sloan Technology Corp.
2. Optical measurements by double spectrophotometer from 0.35 μm to 2.5 μm , to measure integral cover transmittance. The cover films were measured in transmittance on glass witness plates and in reflectance on silicon witnesses.
3. Solar cell output was measured before and after integral cover deposition at simulated Air Mass Zero illumination by Applied Solar Energy Corp. The measurement procedure is discussed in Appendix A.
4. For the case of the mixed oxides ($\text{Al}_2\text{O}_3 - \text{SiO}_2$), the Al/Si ratio was measured by electron microprobe analysis.

4.0 RESULTS

4.1 Deposition of SiO₂ Films. We have deposited SiO₂ films by the plasma oxidation of SiH₄ at rates as high as 1.5 $\mu\text{m}/\text{min}$. The table below describes several representative coating runs which produced thick SiO₂ layers. These films were coated both on fused silica and silicon substrates.

Run No.	Thickness	Coating Rate	Overall Transmittance at 500 nm
1311-047	37.8 μm	1.5 $\mu\text{m}/\text{min}$.	83%
1311-045	2.9	0.48	92.5%
1311-093	3.1	0.28	92.5%
1311-088	23.5	0.13	94% (Fig. 11)
1311-085	9.6	0.37	93% (Fig. 12)
1311-049	3.5	0.55	92.5% (Fig. 13)
1311-087	28.5	0.16	88%
1311-065	16.5	0.15	92.5%
1311-146	50.0	0.13	88%
1311-145	52.0	0.16	90%
1311-144	75.0	0.21	91%

The useful SiO₂ coating rate is limited to about 0.5 $\mu\text{m}/\text{min}$. by film absorption believed associated with oxygen deficiency. The silane oxidation could be improved either by more complete activation of the oxygen in the plasma or by a more favorable SiH₄/O₂ ratio. Relatively clear films are produced when the SiH₄/O₂ ratio is low. Further work is required to relate film absorptance with oxygen activation rate. However, even at 0.5 $\mu\text{m}/\text{min}$., a 100 μm film is produced in 200 minutes, a coating time of practical interest.

If plasma power and oxygen flow rate are fixed, the SiO₂ coating rate depends on SiH₄ flow rate. Figure 14 indicates the stability of SiO₂ coating rate over a three hour period at a fixed SiH₄ flow rate.

OKLI OPTICAL COATINGS
LABORATORY, INC.
2789 Giffen Avenue
Santa Rosa, California
Telephone (707) 545 6440

SPECTRAL PERFORMANCE

DATA IDENTIFICATION OKLI W/O Run No. 1311-088		SAMPLE IDENTIFICATION Filter Type SiO₂ Material FS 146	INST. OPERATING PARAMETERS Resolution Scan Speed 50 Response 0.1 Aperture 570 Expansion 0-100% <input checked="" type="checkbox"/> Percent Transmission <input type="checkbox"/> Percent Reflection	TEST CONDITIONS Time Am.E. Angle 0°	Analyst JW Date 4-11-75 GEARS Vc FRONT 48 BACK X EXPANSION IX PAGE 01
---	--	--	---	---	---

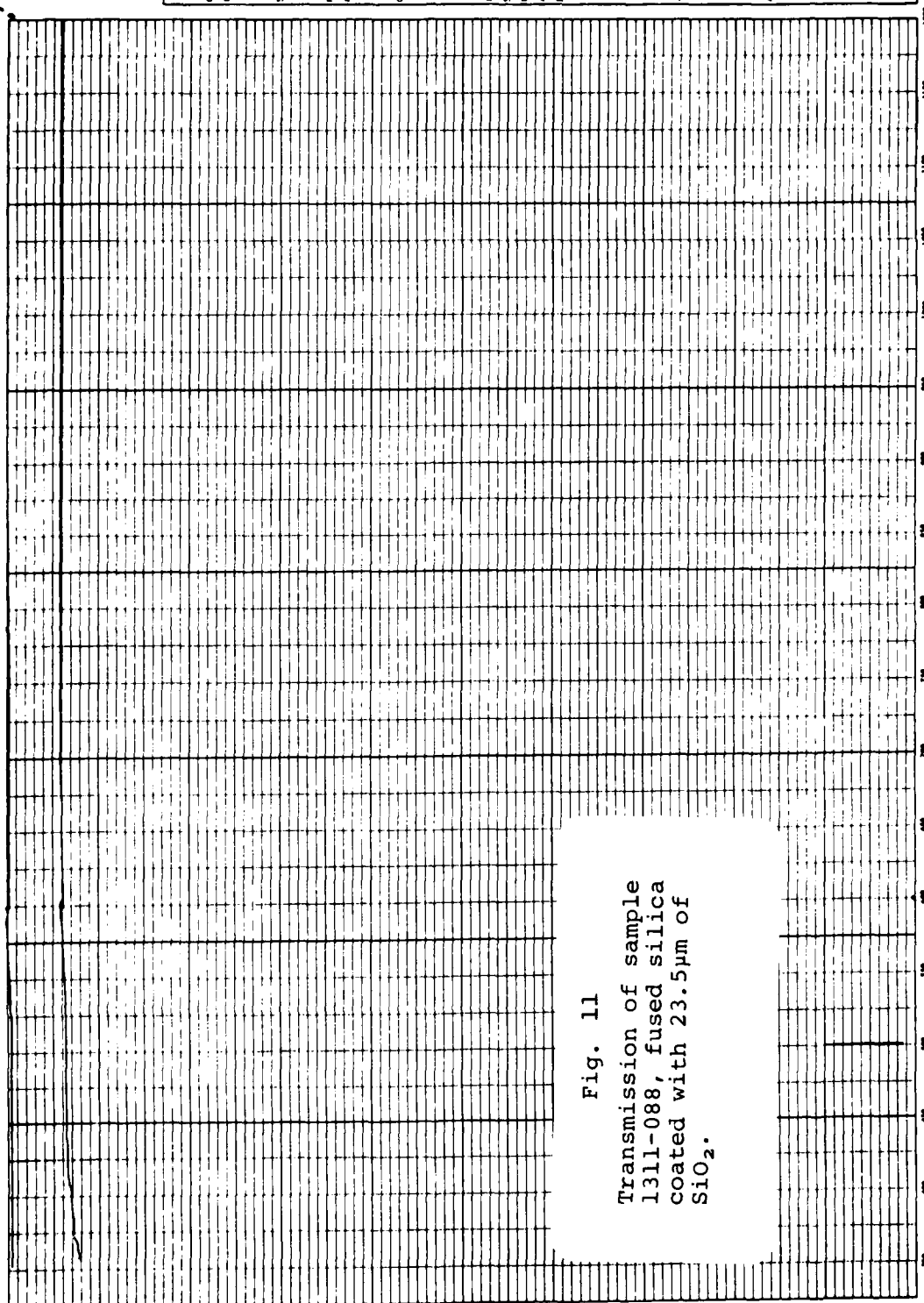


Fig. 11
Transmission of sample
1311-088, fused silica
coated with 23.5µm of
SiO₂.

OKLI 13

OKLI OPTICAL COATINGS
 2780 Giffen Avenue
 Santa Rosa, California
 Telephone (707) 545 0440

SPECTRAL PERFORMANCE

DATA IDENTIFICATION OKLI W/O Run No 1311-085 Serial No (5)		SAMPLE IDENTIFICATION Filter Type Material FS-146		TEST OPERATING PARAMETERS DK-2 Resistor Scan Speed 50 Resolution .01 Aperture STD Exposure 0-1000 OAT <input checked="" type="checkbox"/> Percent Transmission <input type="checkbox"/> Percent Reflection		TEST CONDITIONS Temp AMS Angle 00		Analyst JW Date 11-16-77	GEARS 96 FRONT 48 BACK X EXPANSION 1X PAGE 1 of 1	DATE/LENGTH MILLICENTIMETERS
--	--	---	--	--	--	---	--	--	--	------------------------------

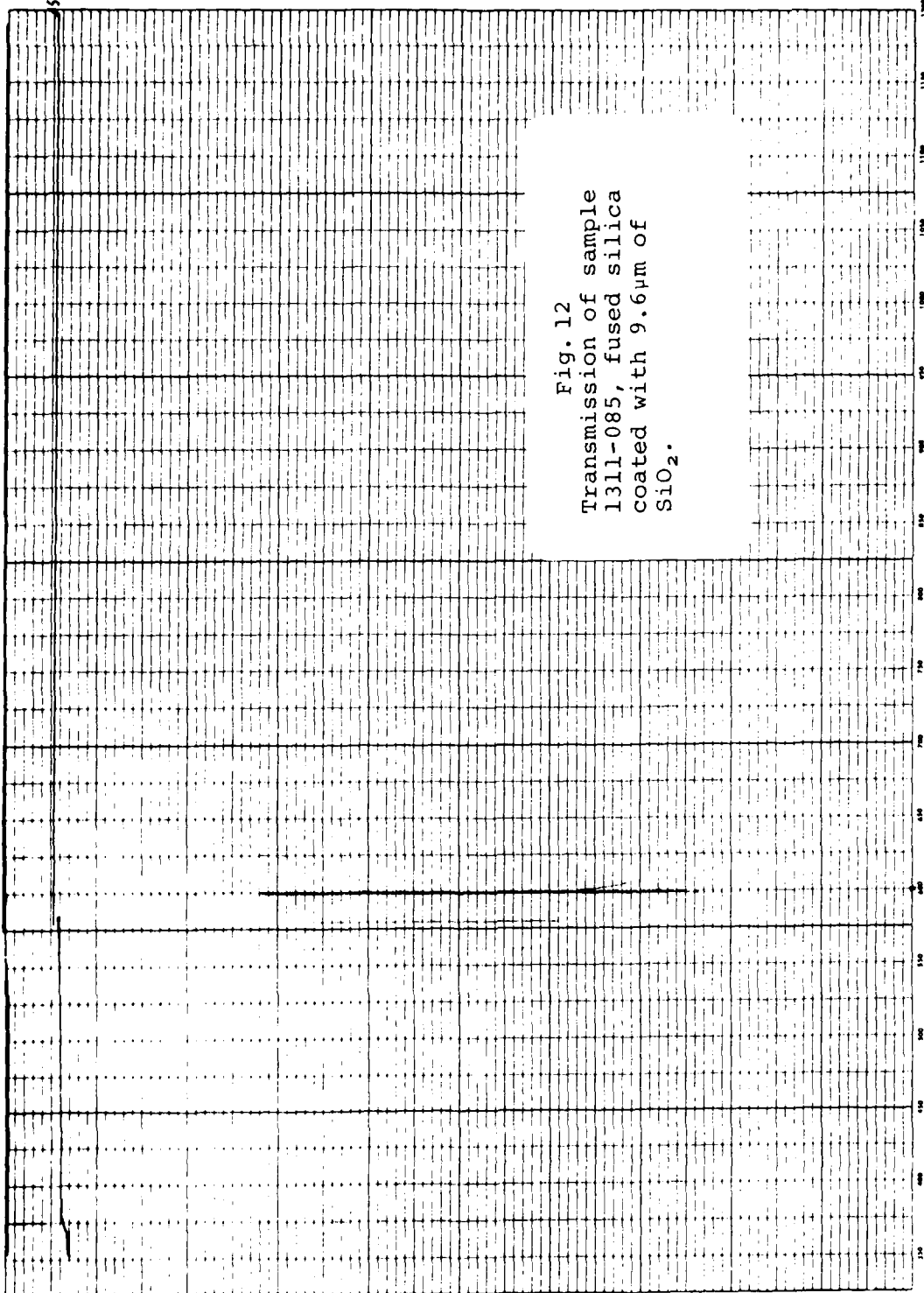


Fig. 12
 Transmission of sample
 1311-085, fused silica
 coated with 9.6µm of
 SiO₂.

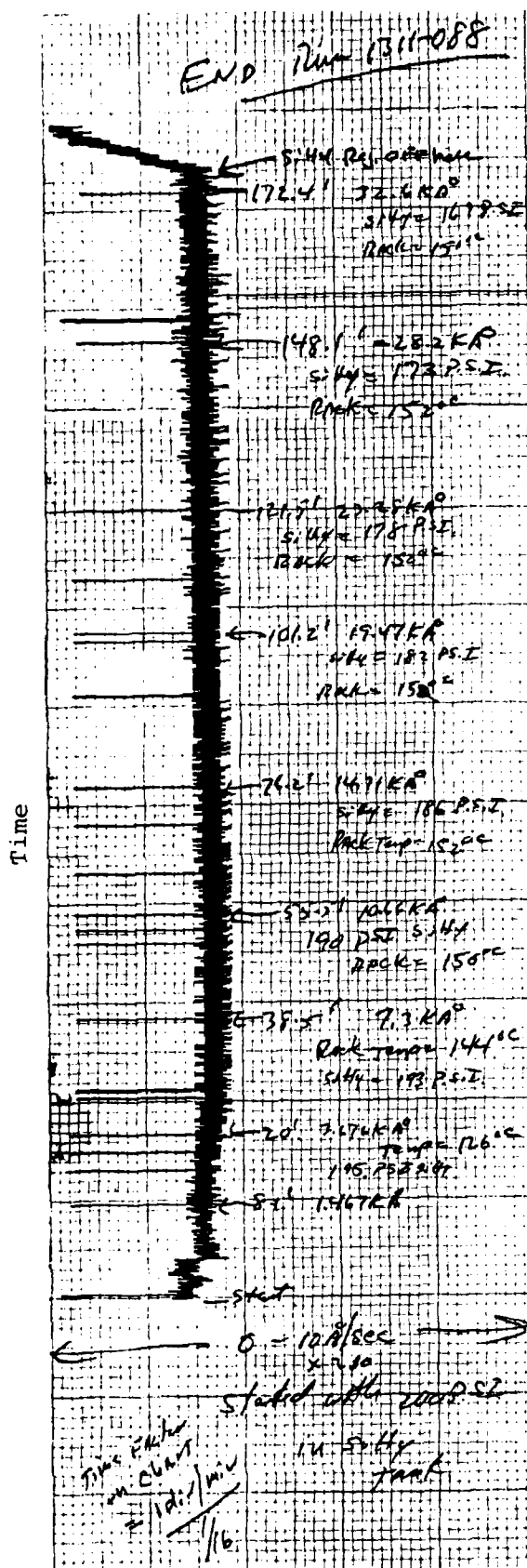
OCL Optical Coatings
Laboratory, Inc.
2789 Gillen Avenue
Santa Rosa, California
Telephone (707) 545-6440

SPECTRAL PERFORMANCE

DATA IDENTIFICATION		OCL No. 1311-049		44 3/60	
Serial No.		Sample Identification		Filter Type S ₂	
Material		Material		F ₂ 1/46	
Configuration		TEST OPERATING PARAMETERS		DK-2	
Resolution		Scan Speed		50	
Response		Aperture		.01	
Exposure		Exposure		370 0-100%	
Percent Transmission		Percent Reflection		0.4%	
TEST CONDITIONS		Temp		AMB	
Angle		Angle		0°	
Analyze		Jaw		Dwell-1675	
GEARS 9% FRONT		4% BACK		X EXPANSION 1X	
PAGE 1		of 1		WAVELENGTH - MILLIMICRONS	

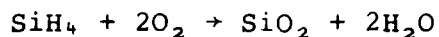
Fig. 13
Transmission of sample
1311-049, fused silica
coated with 3.5μm of
SiO₂.

Fig. 14
Coating rate as measured by
quartz frequency monitor during
run 1311-088.



At fixed oxygen flow, the deposition rate of SiO_2 from silane was dependent on the SiH_4 flow, the total gas flow into the chamber, the position of the silane delivery tube in relation to the source and substrate and, to some extent, the RF power.

1. Deposition rate, as shown in Figure 15, appears to be linearly dependent on the RF power when the ratio of SiH_4 flow rate to O_2 flow rate is 40 cc/min.:50 cc/min. or higher at standard temperature and pressure (run no. 1311-038). At lower ratios (run no. 1311-040), the power dependence is not significant (Figure 16).
2. The deposition rate is shown in Figures 18 and 19 to be dependent on the flow rate ratio of the reactant gases (SiH_4 , O_2). As expected, the rate also appears to increase as the total volume of the gases increases. Considering the reaction in producing silica (SiO_2) by oxidation of silane (SiH_4), the equilibrium flow ratio would be expected to be one part (by volume) $\text{SiH}_4/2$ parts O_2 .



Using our equipment design, equilibrium was approximated when the overall SiH_4/O_2 ratio approached 4/5. As expected, below that ratio, the deposition rate increases linearly with the SiH_4 flow rate (Run No. 1311-043) and higher than 4/5 it was proportional to the O_2 flow rate (Run No. 1311-039).

3. The highest rate of deposition was achieved in Run No. 1311-043 with 75 cc/min.:50 cc/min. ratio (140 angstroms/sec.), though significant absorption was observed. The deposition rate was also affected by

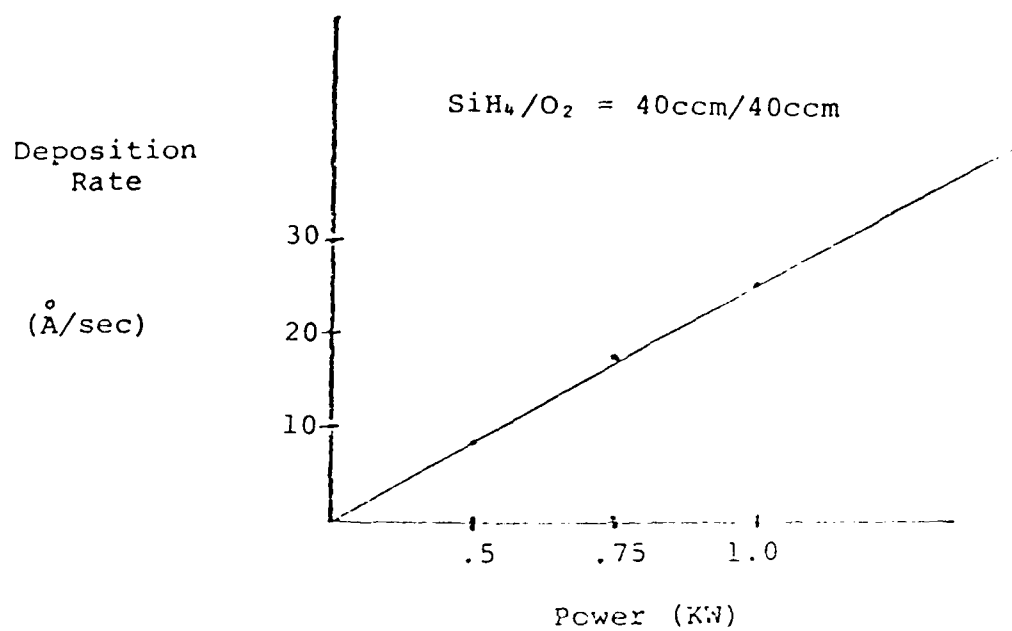


Figure 15
Deposition Rate versus RF Power

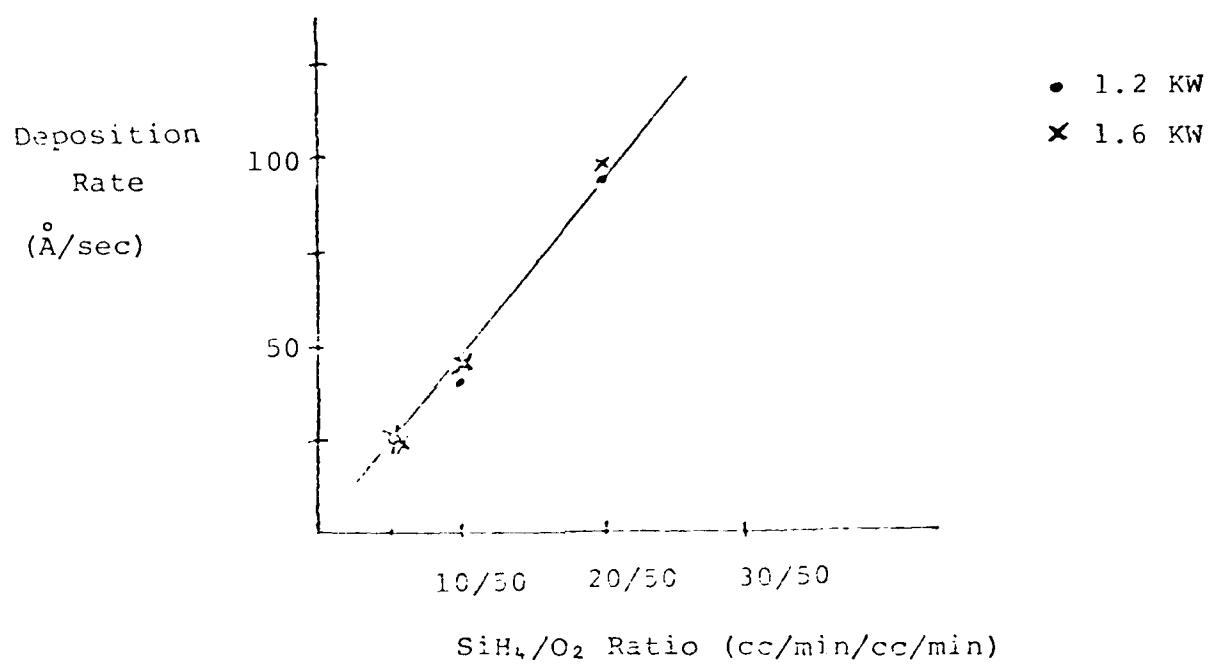


Figure 16
Deposition Rate versus Gas Ratio

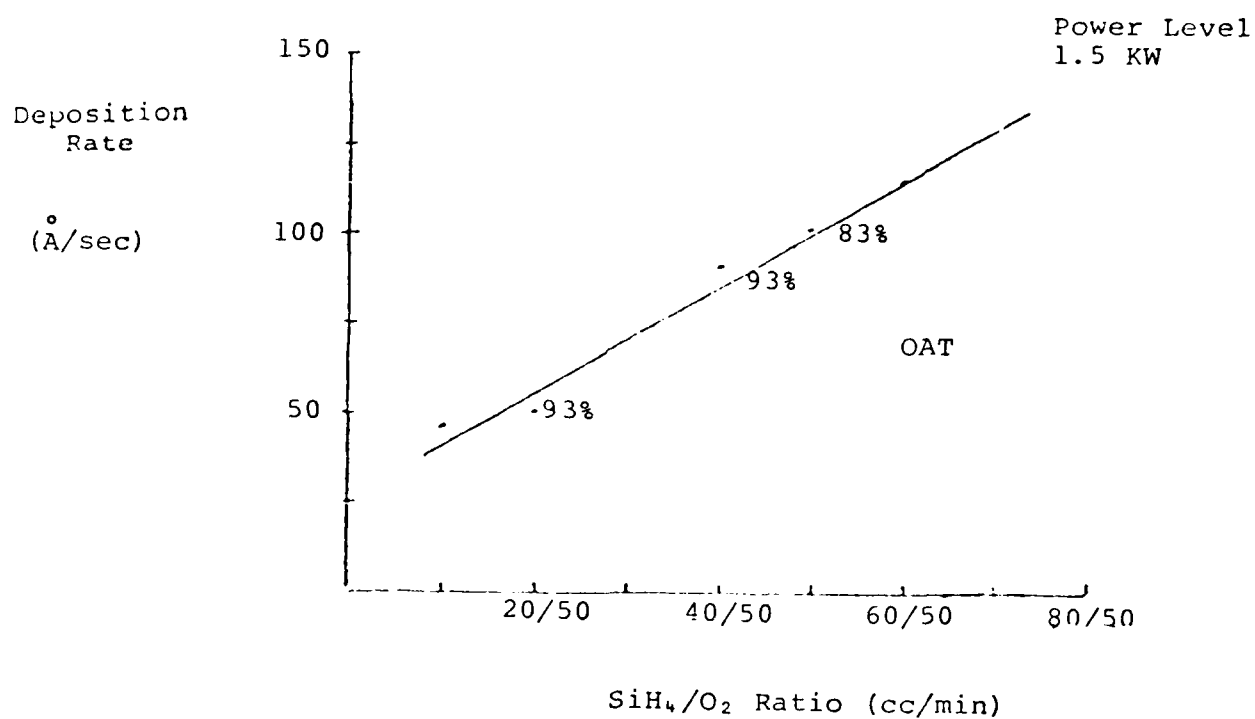


Figure 17
Deposition Rate versus Silane Flow Rate

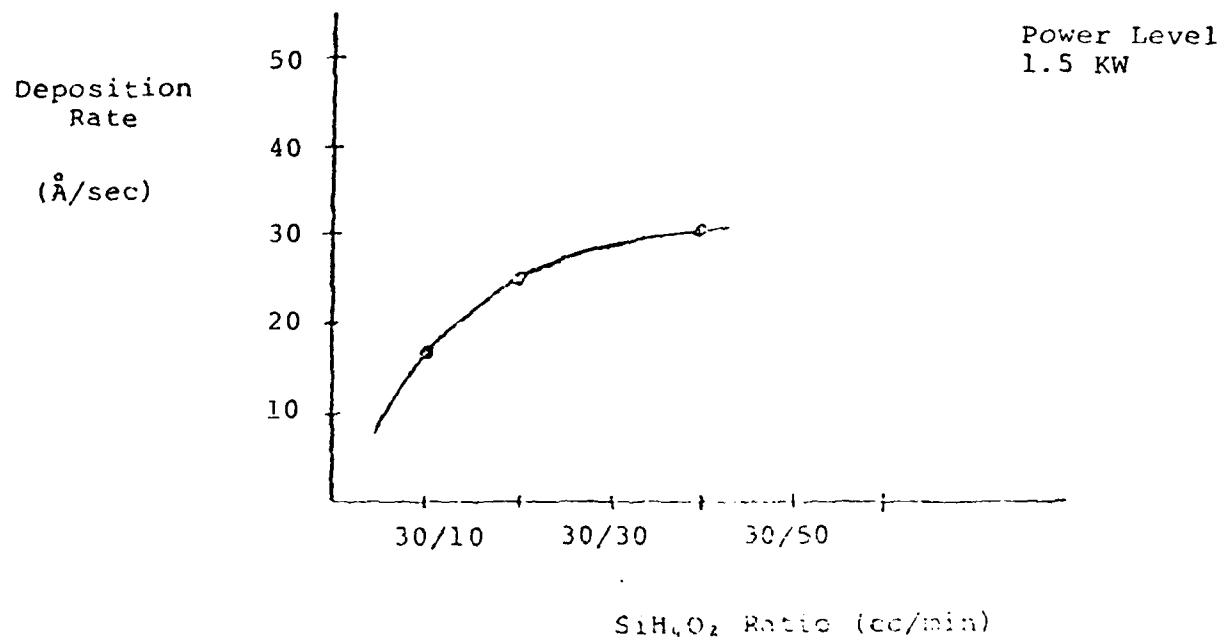


Figure 18
Deposition Rate versus Oxygen Flow Rate

position and design of the silane delivery tube. The schematic in Figure 19 illustrates the gas delivery tube.

The silane tube enters the vacuum chamber external to and above the source that activates the O_2 gas.

According to the data from Run No. 1311-043, -044, and -046 (Figure 20), higher deposition rates resulted with a 5 cm diameter loop in the silane inlet tube (1 mm exhaust holes, spaced $3/4$ inches apart) at a height $5\frac{1}{2}$ cm above the source than at $2\frac{1}{2}$ cm or 8 cm.

Further work with a modified-design inlet tube, Run No. 1311-049, (1.25 cm diameter loop with 1 mm exhaust holes spaced $1/2$ inches apart) resulted in even greater deposition rates. At a height of $2\frac{1}{2}$ cm above the source and with a gas ratio of 30/50 cc/min., the new design tube yielded a rate of 110 angstroms/sec., as compared with the older design with a rate of approximately 55 \AA/sec.

We have dwelt on these process details to illustrate that coating results are quite dependent on apparatus design and the resultant flow conditions. This characteristic is typical of CVD-based processes.

4. The overall transmittance (OAT) is related to the SiH_4/O_2 ratio. As the ratio surpassed $4/5$, the OAT dropped (Run No. 1311-043).
5. As the total volume of gas introduced into the chamber was increased, the deposition rate increased.

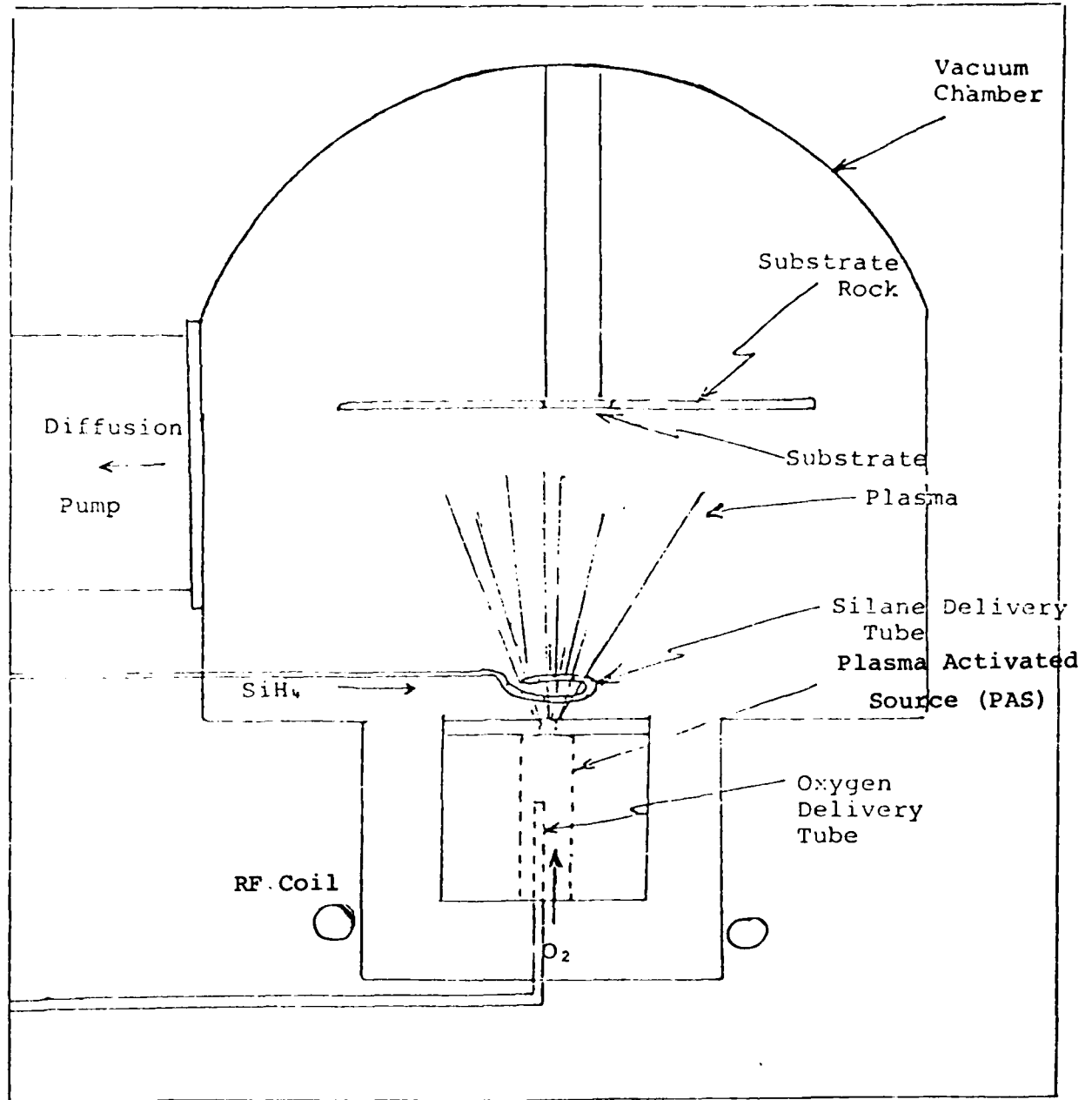


Figure 19
 SiO_2 Deposition Apparatus Schematic

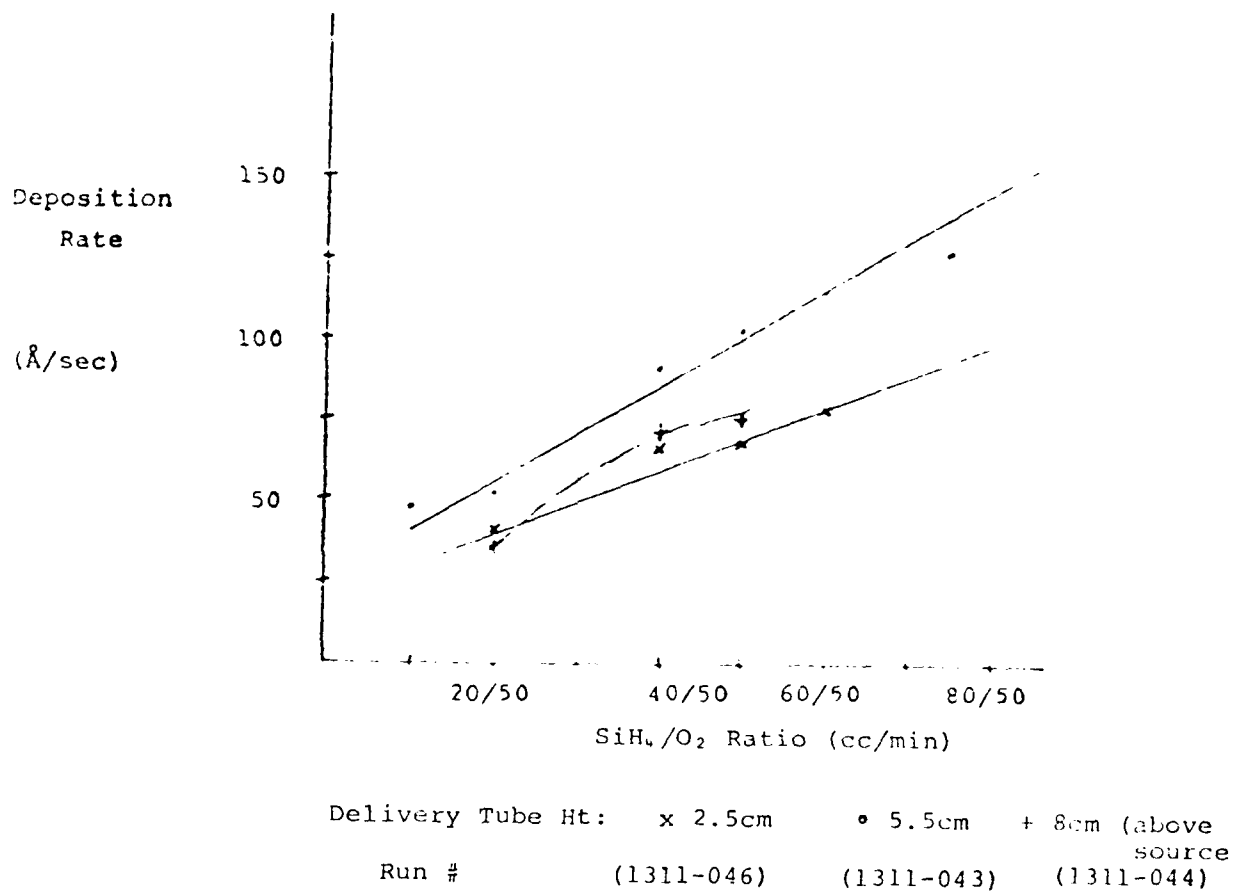


Figure 20
Deposition Rate versus Silane Delivery Tube Height

The thickness variation for SiO_2 deposited onto Si substrates on a plane 21 cm above the PAS source was measured. As plotted in Fig. 21, PAS runoff is considerably less than the typical distribution from a point-source evaporator. Note that thickness runoff is quite small near the origin, thickness falling to 90% of the maximum value when 8 cm from the origin. Hence, at a 21 cm rack height, substrates as large as 16 cm diameter can be coated with 10% runoff or 13 cm diameter with 5% runoff.

On properly cleaned silicon wafers, SiO_2 layers as thick as 130 μm were deposited without delamination or crazing.

• SiO_2 - PAS COATING
 ○ POINT SOURCE
 (HOLLAND, VAC. DEPOSIT.
 OF THIN FILMS, 1963,
 P. 146)

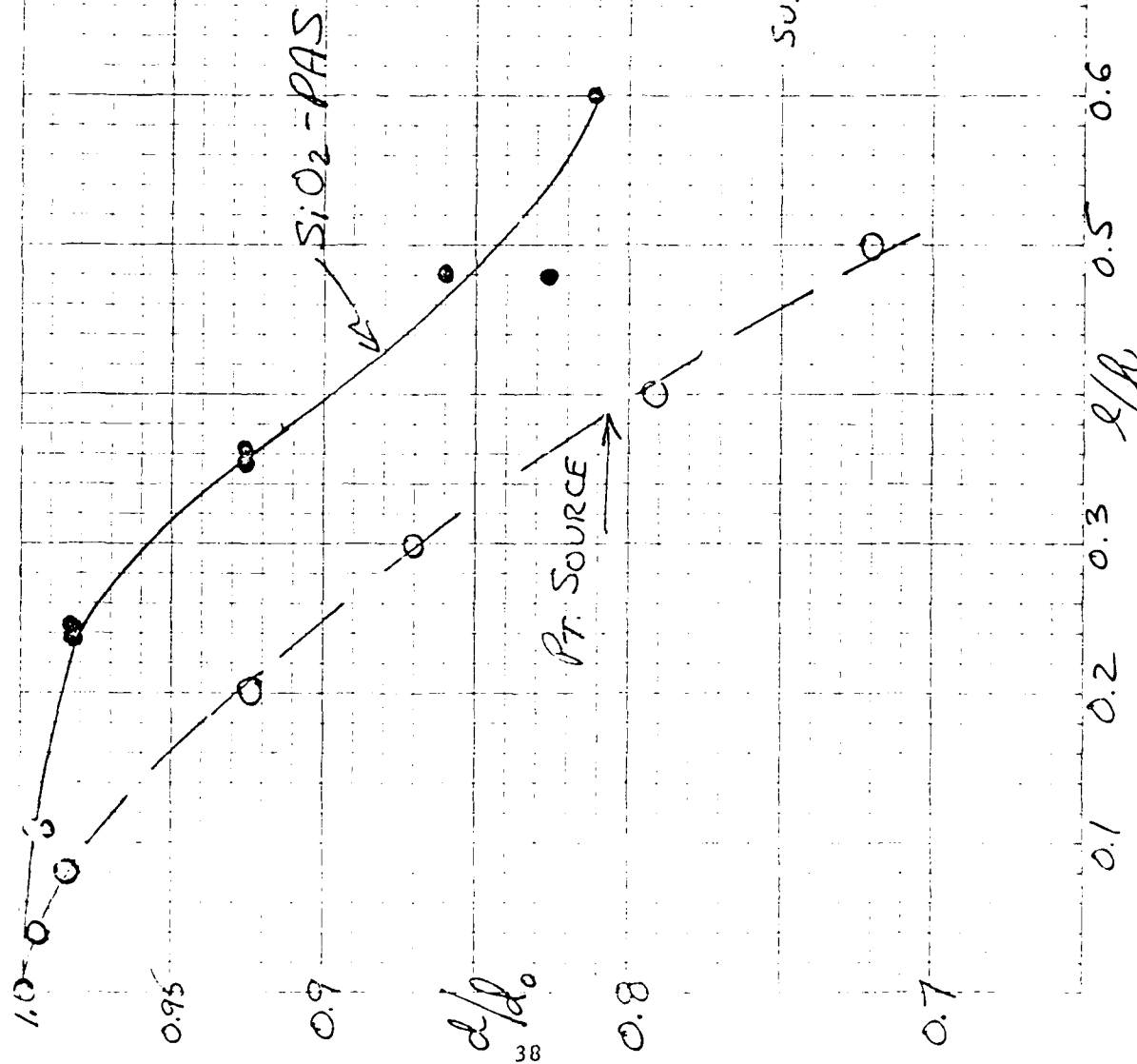
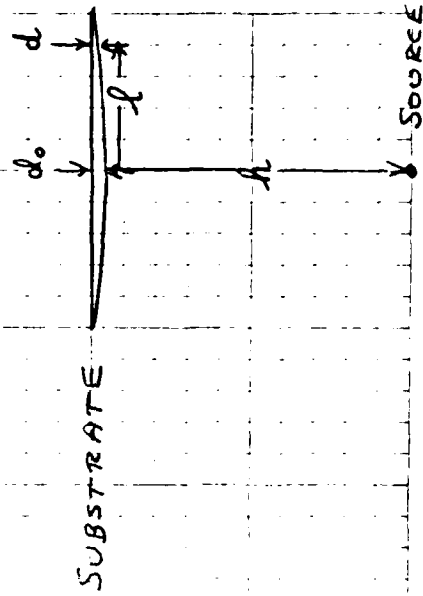


Figure 21. Thickness Distribution



4.2 Deposition of Al_2O_3 from AlCl_3 . The temperature dependence of the vapor pressure of AlCl_3 is shown in Fig. 22. Our experience has indicated that source temperatures of 100-130°C (i.e., $P_{\text{AlCl}_3} \approx 1-15$ mm Hg) are required to coat Al_2O_3 in our PAS system. Al_2O_3 films were deposited at rates as high as 0.5 to 0.8 $\mu\text{m}/\text{min}$. A slowly deposited film 0.077 $\mu\text{m}/\text{min}$. has optical constant values of $n = 1.60$, $k < 0.001$ as determined by ellipsometry at 6328 angstrom wavelength.

One major problem encountered in employing the AlCl_3 route was the Cl_2 evolved by the reaction: $2\text{AlCl}_3 + 3/2 \text{O}_2 \rightarrow \text{Al}_2\text{O}_3 + 3\text{Cl}_2$. Though some films of excellent appearance have been deposited, a definite Cl_2 odor is noticed when the chamber is opened. The presence of substantial quantities of Cl_2 and HCl in the coating apparatus would require careful design of the machine to minimize corrosion damage and environmental problems.

AlCl_3 Route

Run No.	Thickness	Coating Rate	OAT at 500 nm
1311-050	2.5 μm	0.5 $\mu\text{m}/\text{min}$.	91.5% (Fig. 23)
1311-051	0.21	0.066	93%

After preliminary work on this system, we abandoned it for the TEA process because some of the Al_2O_3 films deposited from the chloride corroded badly when exposed to air. These poor films were deposited during runs which had erratic plasmas. Poor control on gas pressure would intermittently extinguish these arcs and result in the incorporation of Cl in the films. With proper control, durable films (such as those listed above) can be obtained. Subsequent work has improved plasma stability by changing source geometry and the pumping system so we could reopen the study of the AlCl_3 system in the future.

Some of the measures which we found to be effective in improving plasma stability include:

1. Avoiding oxygen leaks around the PAS which might permit high pressure regions outside the central orifice.
2. Improvement in the tuning network to minimize power reflected.
3. Running the PAS at a sufficiently high O_2 pressure to maintain ionization.
4. Employing a vacuum system of sufficient throughput to avoid the accumulation of high pressures of early ionized product gases near the PAS.

In short, it is imperative that the O_2 gas within the PAS be the only easily ionized region of the system. If plasma forms elsewhere, it can cause the PAS to be extinguished.

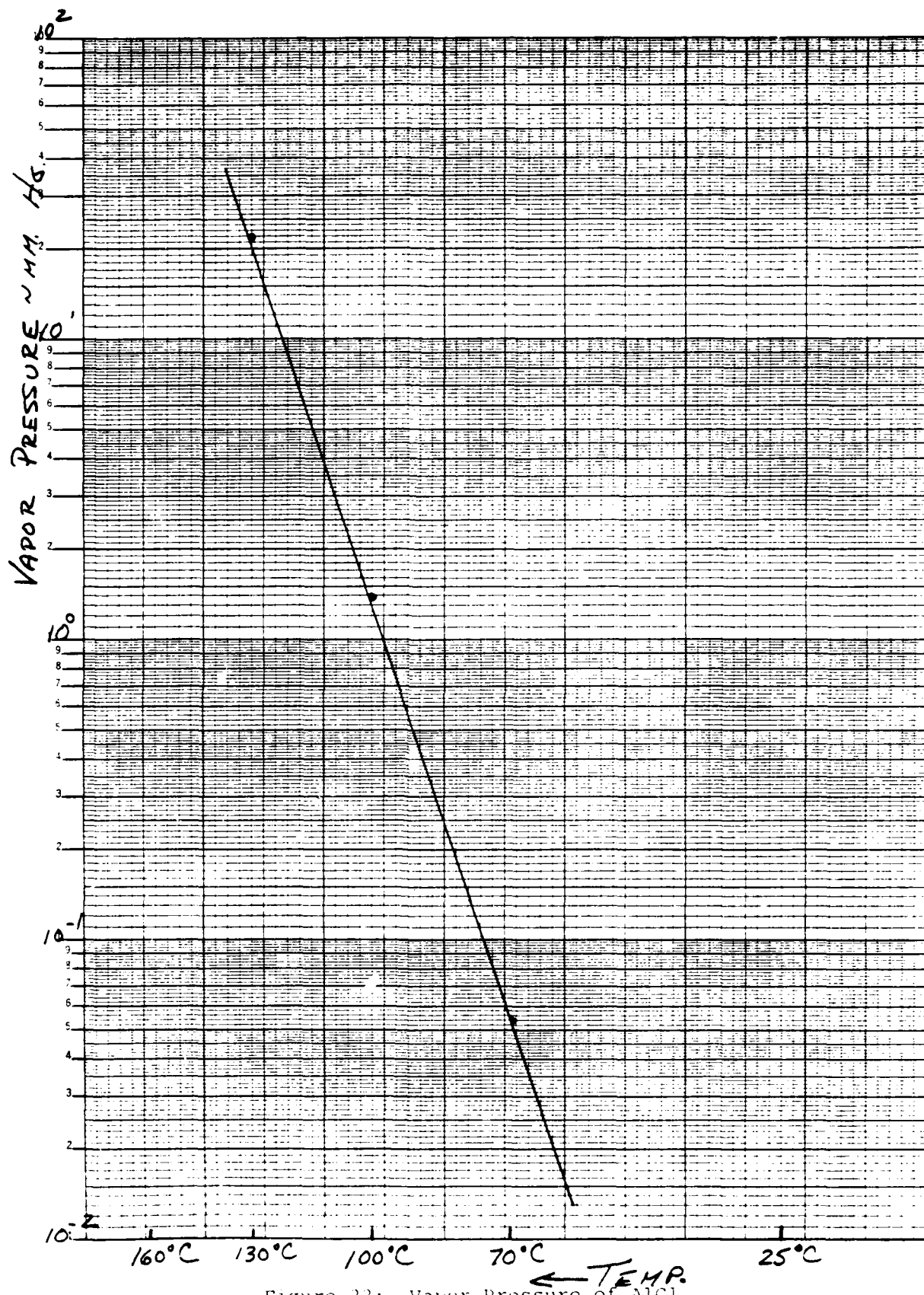


Figure 22: Vapor Pressure of AlCl_3

OCU OPTICAL COATING
UNIVERSITY OF CALIFORNIA
2780 Giffen Avenue
Santa Rosa, California
Telephone (707) 545-6440

SPECTRAL PERFORMANCE

DATA IDENTIFICATION	
OCU W/O	Run No 1311-050
Serial No. #1	
SAMPLE IDENTIFICATION	
File Type	F.S. 146
Material	STRESS 4.2C.
Configuration	
INST. OPERATING PARAMETERS	
DK-2	
Resolution	50
Scan Speed	91
Response	STD
Aperture	0-100%
Exposure	0-100%
Percent Transmission	
<input checked="" type="checkbox"/> Percent Reflection	<input type="checkbox"/>
TEST CONDITIONS	
Time	11:45
Angle	0°
Analysis J.W. 11/6/77	
GEARS 96 FRONT	
48 BACK	
X EXPANSION 1X	
PAGE	1 of 4

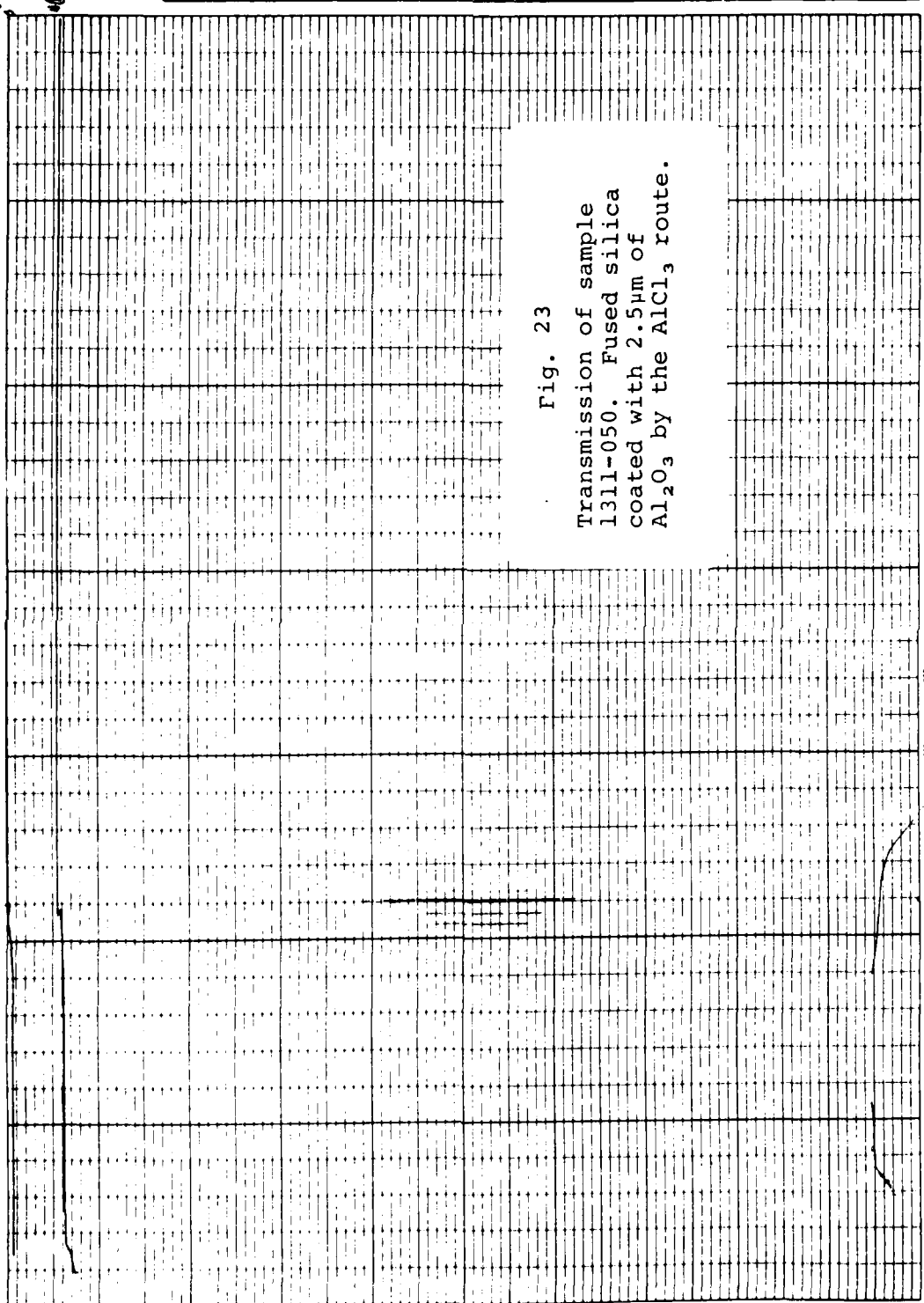
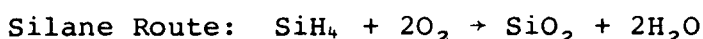


Fig. 23

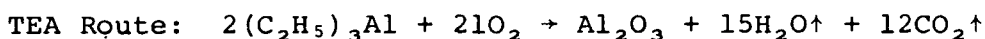
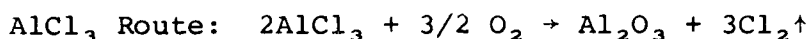
Transmission of sample
1311-050. Fused silica
coated with 2.5µm of
Al₂O₃ by the AlCl₃ route.

4.3 Deposition of Al_2O_3 from Triethylaluminum. Al_2O_3 was deposited successfully from this organo-metallic vapor. In our current equipment, we were limited to coating rates of about 0.3-0.5 $\mu\text{m}/\text{min}$. because of the pumping system's limited throughput capacity for the product gases. The chemical reactions for full oxidation in the coating processes investigated are listed below.

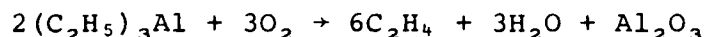
SiO_2 Deposition



Al_2O_3 Deposition



If we assume that an ethene molecule (C_2H_4) is split from the TEA, the product gas volume is appreciably reduced.



The characteristic odor of ethene was quite apparent when the vacuum chamber was opened after a TEA reaction run. A number of other C_xH_y splittings are possible. They all would reduce the product gas load below levels evolved in full oxidation. Mass spectroscopy of reaction gases to correlate the ethene yield with deposition conditions is warranted.

Table 3 compares the moles of oxygen required to deposit one mole of oxide as well as the moles of product gases evolved during coating. If we assume these gases are ideal, the flow rate of each will be proportional to the molar ratio.

Table 3
Gas Requirements for PAS-CVD Coating

<u>Oxide Deposited</u>	<u>Moles O₂ per Mole Oxide</u>	<u>Moles Waste Gas per Mole Oxide</u>	<u>Maximum Coating Rate Achieved</u>
SiO ₂ Silane Route	2	2	1.5 μm/min.
Al ₂ O ₃ AlCl ₃ Route	3/2	3	0.8 μm/min.
TEA Route With Ethene Splitting	21 3	27 9	0.5 μm/min. --

Typical optical characteristics of Al₂O₃ films deposited by the TEA route are listed below:

Run No.	Thickness	Coating Rate	OAT at 500 nm
1311-093	1.91 μm	0.19 μm/min.	90%
1311-092	1.28 μm	0.19 μm/min.	94%

Al₂O₃ coatings thicker than 2-3 μm were all crazed (Fig. 24) when deposited on silicon wafers. Thinner coatings were specular, well adhered and transparent.

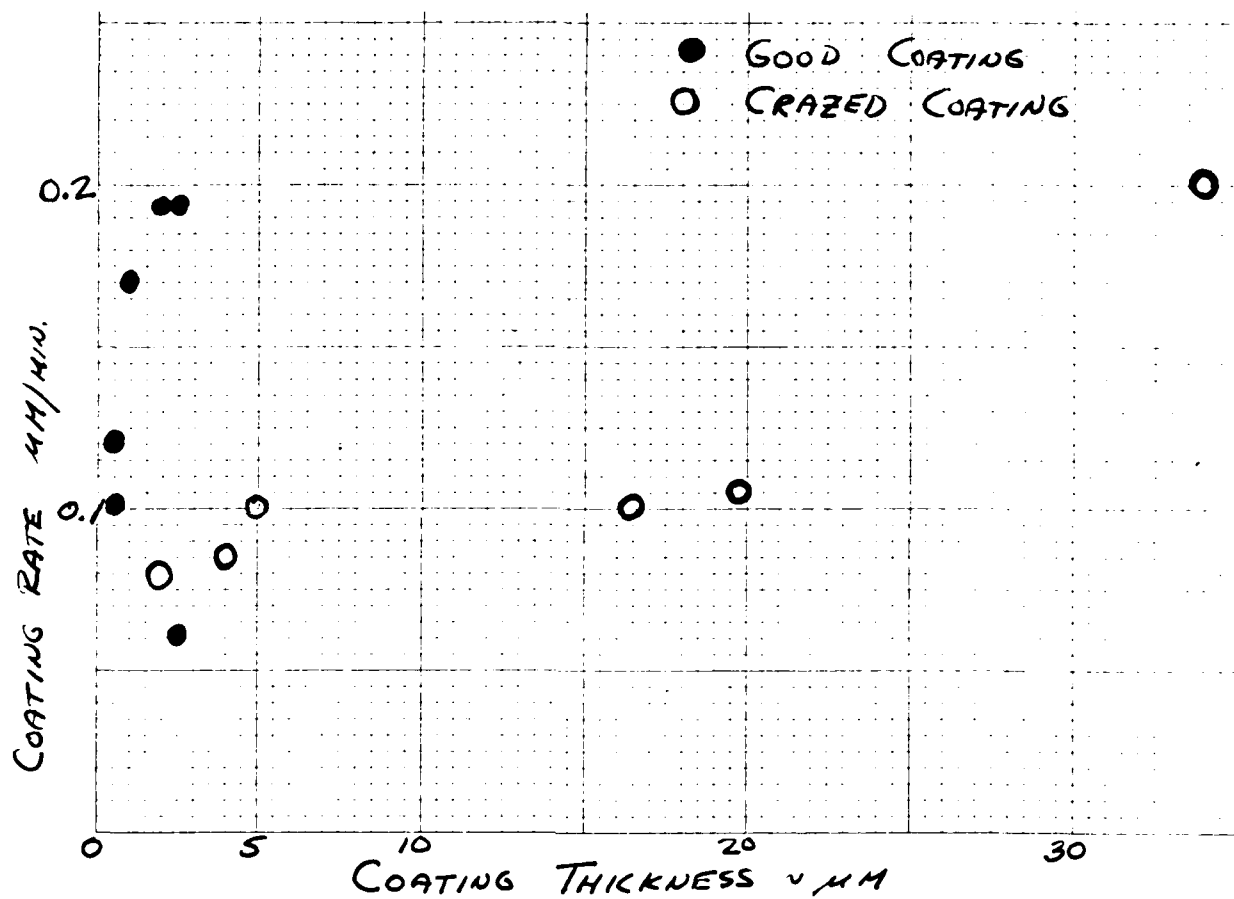


FIG. 24: CRAZING OF Al_2O_3 COATINGS
ON SILICON SUBSTRATES

4.4 Deposition of Mixed SiO_2 - Al_2O_3 Films. Fig. 25 indicates the apparatus used to deposit the mixed oxide films. The silane, being a vapor at room temperature, was metered with a mass flow meter through an injection nozzle located just above the oxygen plasma source. To develop sufficient vapor pressure, the liquid TEA was heated to the 100-120°C range. The vapor flow rate was controlled with a micrometer needle valve. For proper process control, the temperature of the entire TEA gas flow system must be held within close control. Condensation will occur wherever line temperature falls below source temperature and if line temperature exceeds 150-160°C, the TEA will polymerize to form a solid product which will block gas flow.

With our present apparatus, we have no direct measure of TEA flow rate. To control the $\text{SiO}_2/\text{Al}_2\text{O}_3$ ratio, an indirect method was employed.

1. The dependence of SiO_2 coating rate on SiH_4 flow rate was measured directly.
2. The dependence of Al_2O_3 coating rate on TEA source temperature and micrometer valve setting was determined.
3. The deposition of $\text{SiO}_2/\text{Al}_2\text{O}_3$ mixed film was assumed to be an additive process.

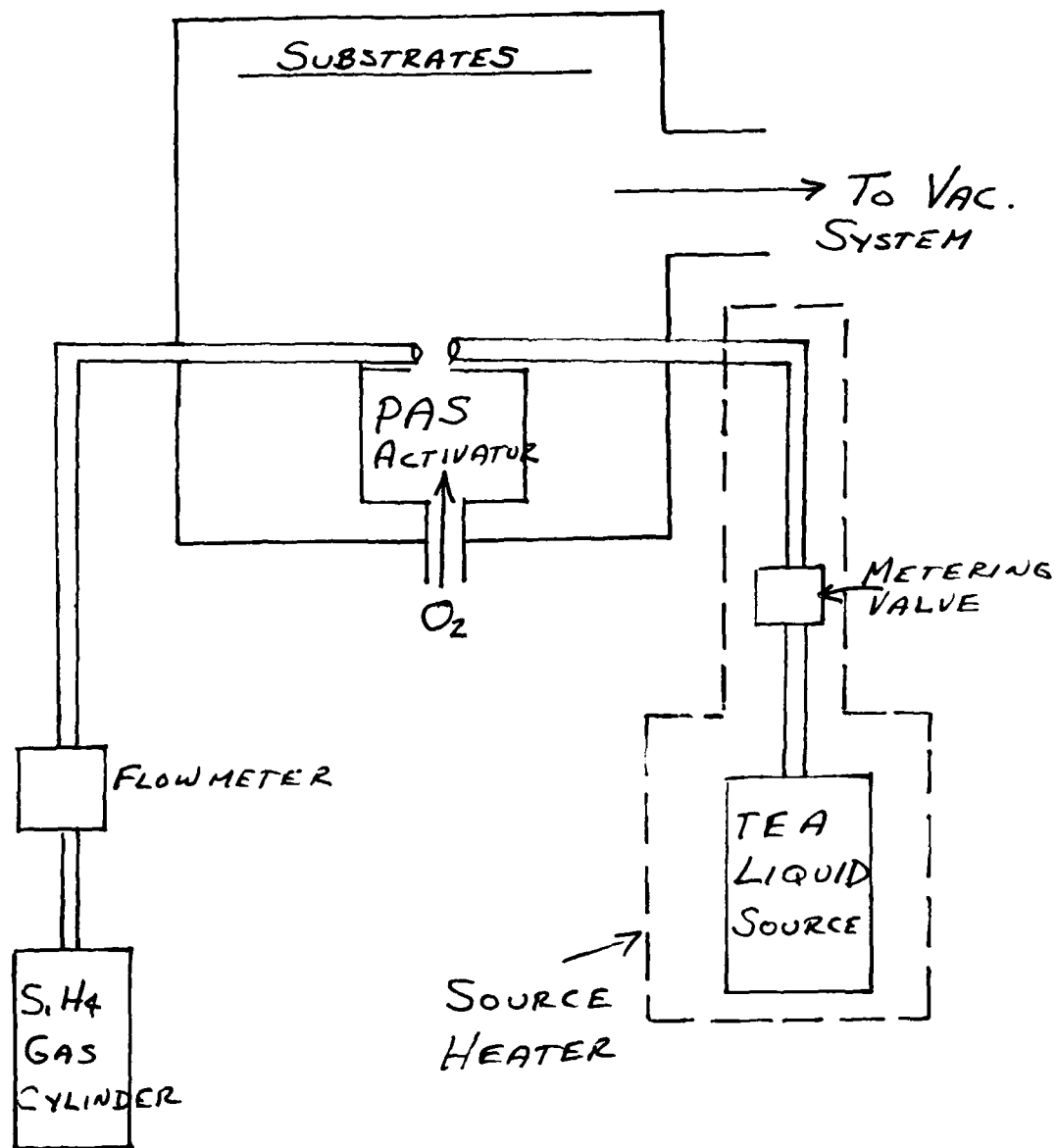


FIG. 25: APPARATUS FOR DEPOSITING $\text{Al}_2\text{O}_3\text{-SiO}_2$ MIXTURES BY TEA-SILANE ROUTE

Typical results of mixed oxide runs were:

Run No.	<u>Al₂O₃</u>		Film Thickness	Coating Rate	OAT at 500 nm
	SiO ₂	+ Al ₂ O ₃ * **			
1311-093		0.45	7.4 μ m	0.5 μ m/min.	83%
1311-092		0.1	0.78	0.14	90%
1311-092		0.1	7.85	0.15	89%
1311-095		0.1	5.0	0.18	94% (Fig. 27)
1311-094		0.2	5.4	0.3	85%
1311-097		0.1	14.0	0.28	88%
1311-093		0.1	13.5	0.11	92%
1311-123	0.4	0.55	46.0	0.26	83%
1311-125	0.3	0.5	20.0	0.124	92%
1311-124		0.2	24.3	0.28	20%

* As estimated from reactant gas ratio.

** As measured by electron microprobe analysis
(energy dispersive X ray fluorescence method).

The crazing noted in the Al₂O₃ coatings (see Fig. 24) was apparently reduced in Al₂O₃ - SiO₂ mixed oxides (Fig. 26). Crazing occurs when film thickness exceeds 15-18 μ m and does not appear to depend on Al₂O₃ fraction over the range tested.

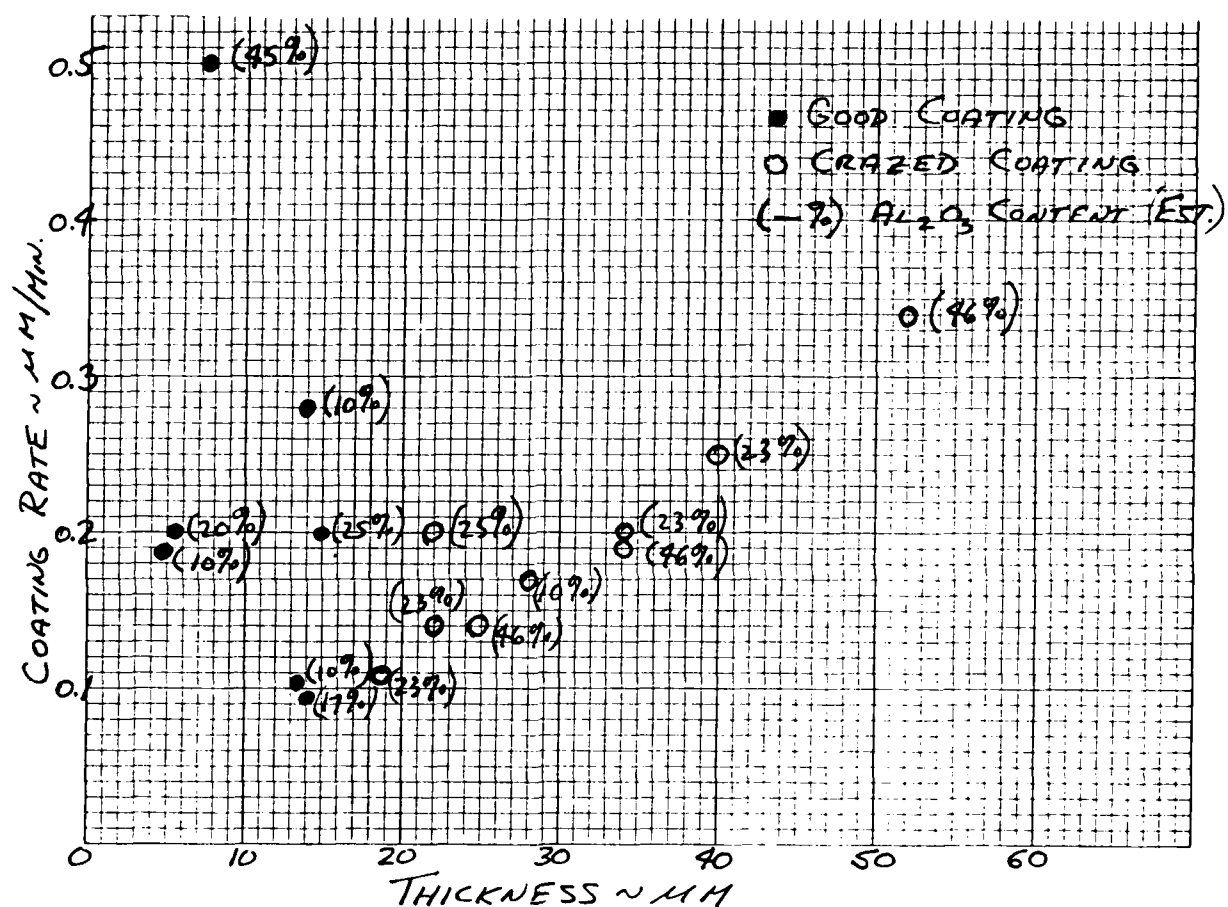


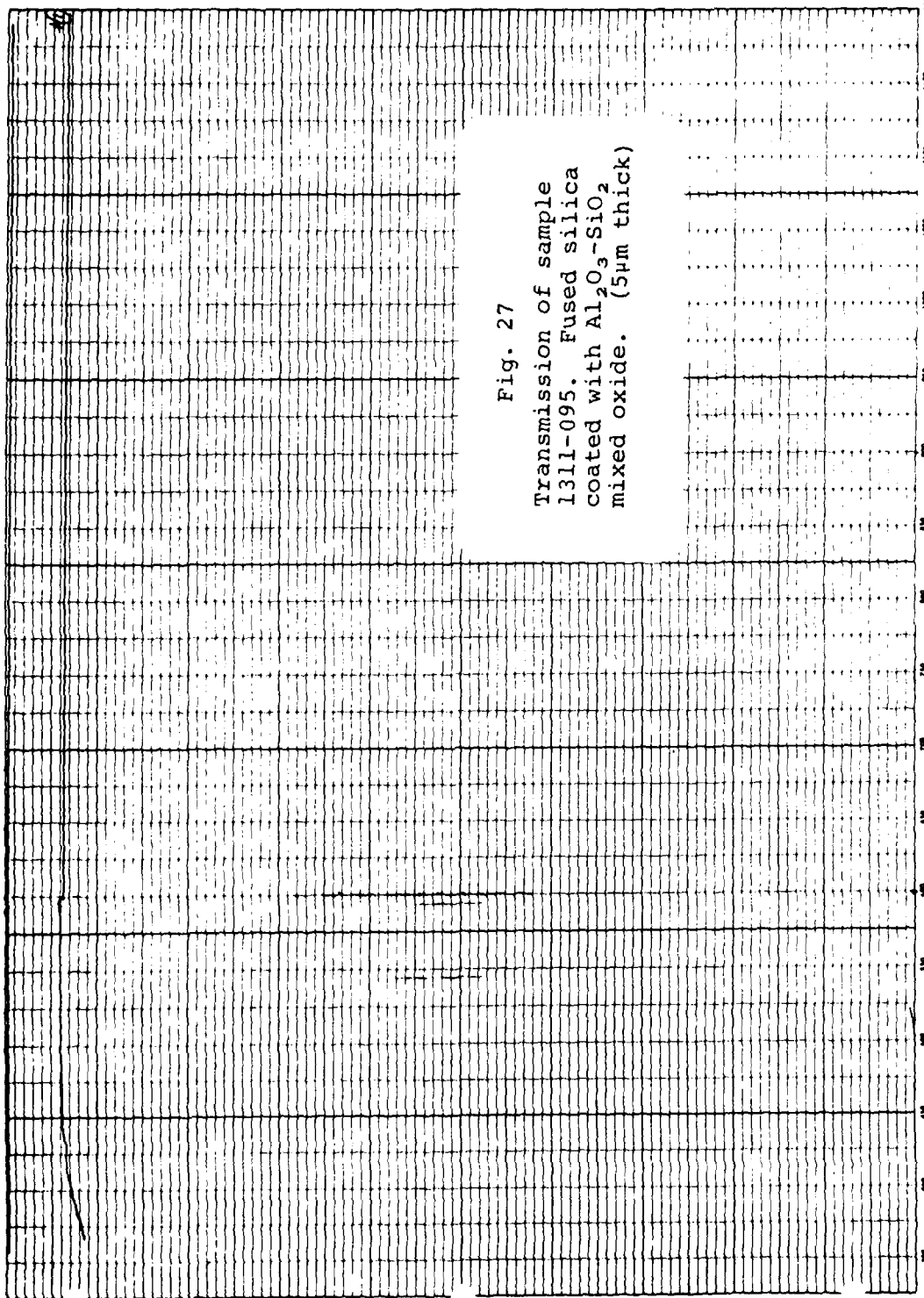
FIG. 26: CRAZING OF $Al_2O_3-SiO_2$ FILMS
ON SILICON SUBSTRATES

OCU 12

OCU OPTICAL COATING
LABORATORY INC.
2799 Giffen Avenue
Santa Rosa, California
Telephone (707) 545 6440

SPECTRAL PERFORMANCE

DATA IDENTIFICATION	
OCU W/O	Run No 1311-095
Serial No	#1
SAMPLE IDENTIFICATION	
Filter Type	T-50/6.44/μ
Material	F-5 146
Configuration	
TEST OPERATING PARAMETERS	
DM-2	
Resolution	50
Scan Speed	0.1
Retardance	STD
Aperture	0-100% T
Exposure	0.5 sec
Percent Transmission	0.5 sec
Percent Reflection	0.5 sec
TEST CONDITIONS	
Temperature	100° R
Humidity	0-100%
ANALYST JW Date 11/16/77	
GEARS 90 FRONT 45 BACK X EXPANSION 1X	
PA-1	91



4.5 SiO₂ Coatings on Silicon Solar Cells. The 10-12 mil thick solar cells coated were all obtained from Applied Solar Energy Corp. (ASEC) and can be classified into several groups.

1. Standard solar cells with either MLAR or single layer AR coatings.
2. High efficiency, violet solar cells with MLAR coatings.
3. Textured cells with no AR.
4. Polished cells with no AR.

We took advantage of the reproducible thickness runoff across the stationary substrate holder rack to coat a series of cells with a range of SiO₂ cover thicknesses in each run. (To assure cell cover thickness uniformity in a production mode, the cell holders would customarily be rotated.)

When cooled after coating, a number of cells fractured from the intrinsic coating stresses. Figure 28 presents the incidence of failure as a function of cover thickness. Note that a large fraction of cells with covers between 75 and 100 μm thick did not fail. Indeed, the thickest cover, 130 μm , did not fracture its cell. Fracture was delayed for days after coating in several cases. We found that, among the later runs, Runs 145, 146, 147 were all significantly more fracture resistant than 143 or 144, but we cannot yet relate the difference to coating process parameter differences.

After coating, the residual deposition stresses dish the cells with the SiO_2 on the convex side (hence the SiO_2 cover has residual compressive stress). The magnitudes of the residual stresses were compared by measuring peak deflection at the center of each cell with a depth microscope. As shown in Fig. 29, the stresses in cells from Runs 144-147 exhibited stresses which have a common dependence in SiO_2 thickness. As might be expected, Run 143, which had the worst fracture resistance, showed higher stresses.

We have concluded that there is a high probability that silicon cells can be coated in a production process with SiO_2 covers over 75 μm thick without fracture. The operative problem is the effect of cell curvature on array assembly and long-term performance. The difficulty of assembling deformed cells could be minimized by assembly prior to coating. Coating of assembled subarrays would have two incidental benefits.

- A. The labor required to load and unload the coater would be minimized.
- B. The need to mask contact pad areas to avoid plasma oxidation of the metallization would be avoided by interconnecting them prior to cover deposition.

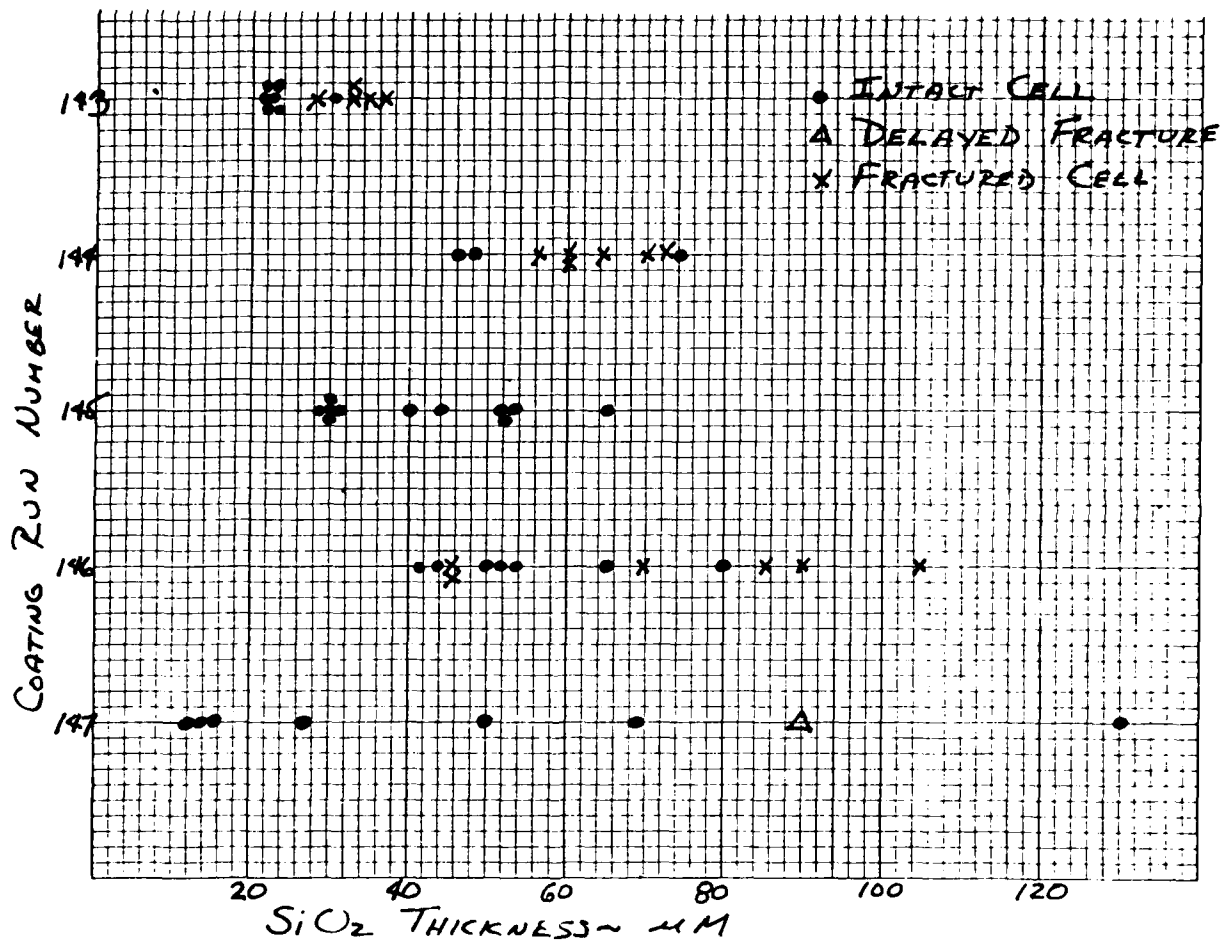


FIG. 28: FRACTURE OF SILICON SOLAR CELLS AFTER PAS-SiO₂ COATING

The change in electrical performance due to coating is tabulated in Table 4. Note that there is little change in V_{oc} or in fill factor. I_{sc} decreases with PAS cover deposition, but the loss appears to be independent of SiO_2 thickness. We believe this drop in short circuit current is due to optical mismatch in the SiO_2 covered cells which can be readily corrected by proper index matching AR stacks. Cell output prior to coating was measured on uncovered cells. The addition of a fused quartz plate cover in optical contact dropped I_{sc} by about 1.5%.

The changes in electrical output of a series of textured silicon cells, which had no AR coating are tabulated in Table 5. Unlike the polished MLAR-coated cells, both fill factor and I_{sc} were degraded by the integral SiO_2 covers. As SiO_2 thickness increases, the loss in I_{sc} first rises to about 30 ma and then falls to zero when the cover is 130 μm thick. On the other hand, the loss in fill factor generally gets more severe as SiO_2 thickness is increased.

TABLE 4
ELECTRICAL OUTPUT OF PAS COATED SILICON SOLAR CELLS
(HIGH EFFICIENCY VIOLET CELLS)

<u>SiO₂ Thickness</u>	<u>I_{sc}</u>	<u>V_{oc}</u>	<u>f.f.</u>	<u>Loss in I_{sc}</u>
As received	177 ma	0.600 V	0.754	9.0%
with 25 μ m	161	0.595	0.772	
22.5	176	0.605	0.748	8.5
	161	0.597	0.770	
22	172	0.605	0.772	6.4
	161	0.598	0.771	
28	160	0.590	0.770	2.5
	156	0.590	0.750	
31	172	0.600	0.775	2.9
	167	0.600	0.761	
31	170	0.590	0.732	1.1
	168	0.589	0.720	
35	168	0.595	0.760	1.8
	165	0.593	0.770	
40	168	0.590	0.760	5.0
	160	0.590	0.760	
47	172	0.600	0.769	4.6
	164	0.595	0.758	
48	157	0.590	0.790	5.7
	148	0.590	0.760	
63	161	0.590	0.771	6.2
	151	0.597	0.775	

TABLE 5
ELECTRICAL OUTPUT OF PAS COATED TEXTURED SILICON
SOLAR CELLS (NO AR ON CELLS)

<u>SiO₂ Thickness (μm)</u>	<u>As Coated</u>			<u>Before Coating</u>			ΔI_{sc}	$\Delta f.f.$
	I_{sc}	V_{oc}	f.f.	I_{sc}	V_{oc}	f.f.		
23	143	550	66.4	159	575	78.5	16	12.1
23	143	565	72.4	159	575	78.5	16	6.1
23	139	580	71.1	160	580	76.0	21	4.9
31	128	560	71.6	159	580	77.6	31	6.0
31	137	565	68.0	160	580	75.5	23	7.5
40	142	560	73.6	159	580	77.6	17	4.0
52	139	580	70.4	160	580	75.5	21	5.1
52	133	557	74.3	158	590	78.0	25	3.7
70	158	555	66.0	161	590	75.8	3	9.8
74	158	567	69.0	160	585	76.7	2	7.7
130	161	550	64.0	161	590	75.8	0	11.8

4.6 SiO₂ Coatings on GaAs Solar Cells. SiO₂ was coated on GaAs cells using the same procedure employed for Si cells. The cells coated are listed in Table 6.

In general, our results indicate that SiO₂ covers thicker than about 40-50 μ m fractured the GaAs cells. Thermal stressing of the GaAs cells (Table 7) indicated that even uncoated cells failed by either delamination of the AR layer and/or cell cracking. Hence, it is not surprising that the stress induced by thick SiO₂ layers caused cell fracture.

Because of these preexisting defects in the limited number of GaAs cells available to this program, meaningful data on the effect of SiO₂ coating on electrical characteristics could not be obtained.

TABLE 6
PERFORMANCE OF COATED GaAs CELLS

	<u>Cell No.</u>	<u>SiO₂ Thickness</u>	<u>Fractured During Coating</u>	<u>Fractured After Coating</u>
Practice Cells	4114	16 μm	No	No
	4111	32 μm	No	
		Added 50 μm	Yes	
	4043	25 μm	No	Failed in Thermal Cycle
	4037	35 μm	No	Failed in Thermal Cycle
	4038	45 μm	No	
		Added 25 μm	Yes	
Deliverable Cells	4127	40 μm	Yes	
	4179	75 μm	Yes	
	4165	55 μm	Yes	
	4181	55 μm	Yes	
	4133	35 μm	No	Failed in Handling
	4185	40 μm	Yes	

TABLE 7

Thermal Shock Resistance of GaAs Cells

<u>Type of Cells</u>	<u>SiO₂ Thickness</u>	<u>Thermal Cycle</u>	<u>Results</u>
<u>GaAs</u>			
"Practice" cells			
4051	None	300°C/LN ₂ 1 cycle	AR coating lifting in 1/2- 2 mil "measles"
4043	25μm	300°C/LN ₂ 1 cycle	AR coating and SiO ₂ both lifting in scattered 1/2 mil "measles"
4043	25μm	400°C/LN ₂	More SiO ₂ lifting.
4111	32μm	150°C/LN ₂ 10 cycles	Random measles appeared at sixth cycle, did not spread.
4057	35μm	150°C/LN ₂ 10 cycles	Had random measles before cycling. No further degra- dation.
<u>GaAs</u>			
Deliverable cells			
4127	None	RT/LN ₂ one cycle	Scattered "measles" Several cracks in each sample extend- ing into cell.
4181			

5.0 CONCLUSIONS

5.1 The Plasma Activated Source (PAS) can continuously deposit transparent SiO_2 integral covers as thick as $130\text{ }\mu\text{m}$ at rates above $20\text{ }\mu\text{m/hr.}$ at Si cell temperatures well below 150°C.

5.2 The integral SiO_2 covers do not crack or craze if the substrate is properly cleaned. However, the intrinsic coating stresses do dish the cells, with the cover in compression. Cell stress depends on SiO_2 thickness and, with one exception, was not dependent on coating parameters. In general, coatings thinner than $50\text{ }\mu\text{m}$ did not cause cell fracture. Above $50\text{ }\mu\text{m}$ thickness, cell fracture was occasionally noted, although cells as thickly coated as $130\text{ }\mu\text{m}$ survived intact.

5.3 The addition of Al_2O_3 to the cell cover coating changes its stress to strongly tensile. Pure Al_2O_3 covers craze when they are thicker than about $3\text{ }\mu\text{m}$, and 20% Al_2O_3 -80% SiO_2 covers craze when thicker than $20\text{ }\mu\text{m}$. Coating stress reduction at the compressive-to-tensile crossover is expected to occur near 5-10% Al_2O_3 . Coating apparatus modification is required to reproducibly coat this critical mixture.

5.4 The deposition of thick SiO_2 integral covers on high efficiency silicon solar cells produces little change in V_{oc} or fill factor. The reduction in I_{sc} does not appear to depend on coating thickness or coating time. Since cell performance is being compared to bare cells, the optical mismatch of the cover could be improved.

5.5 GaAs cells can be coated with SiO_2 covers as thick as 50 μm by this process. Preexisting cell defects (poor AR layer adhesion and GaAs cracking) caused failure of coated cells and prevented fuller evaluation of the integral cover coatings.

APPENDIX A

The ASEC AMO simulator is described under three headings: the light sources and calibration, the cell holding fixtures and the readout equipment.

1.0 LIGHT SOURCES AND CALIBRATION

The AMO spectrum is simulated by two separate sources:

- The blue portion of the spectrum is obtained from a xenon arc lamp with an absorption filter which attenuates the large energy spikes in the near IR region.
- The red portion of the spectrum is due to a tungsten lamp set at 2800°K color temperature with suitable filters to blend with the blue portion of the spectrum, resulting in close approximation to the AMO spectrum. Figure A-1 shows the Johnson AMO spectrum (approximates closely the Thekaekara spectrum) and also the output of the ASEC simulator. Also shown are the separate xenon (blue) and tungsten (red) contributions.

The two light sources do not provide collimated light. The cell test plane is placed at the plane of correct convergence; the uniformity across this plane is $\pm 2\%$ for areas up to 8 cm². The deviation of the centerline of each light source from perpendicular is around 11°.

In addition to allowing cell characterization under the AMO spectrum, this simulator has an added advantage for cell evaluation. By use of suitable blocking shields, either the blue or the red spectral output shown in Figure A-1

can be used to illuminate the cell. Analysis of the absolute output under these two filters can provide a rapid indication of the process control achieved on the cell. Experience has provided guidelines for "typical" readings in these two broadband regions for a variety of cells (including intentional variations in the silicon resistivity, diffusion conditions, surface finish, contact area coverage and whether or not the cell surface has an AR coating). Thus, evaluation of the blue response can indicate the performance of a given diffusion schedule with a given resistivity silicon, and can also check the effectiveness of an AR coating. The red response can also indicate whether the final bulk output is as expected, and can thus be used to assess the minority carrier diffusion length (D.L.) achieved. Although separate methods (surface or bulk photo voltage) are used for diffusion length measurement, this broadband check is most valuable to indicate the possible range of the diffusion length. For low diffusion length values, the red response decreases and crosses over the blue response for $D.L. \approx 10 \mu m$. Thus, the red response data are most useful for scanning a larger number of samples, and can then be related to more precise D.L. values obtained by more detailed (separate) measurements.

1.1 Calibration. When first constructed, the AMO simulators were calibrated by a set of standard cells which were calibrated regularly on Table Mountain by measuring the solar spectrum incident there and by adjusting for the measured absorption band in the spectrum, extrapolating to AMO readings. Since then, it has become common practice to use balloon flown and recovered standard cells to set the AMO simulator intensity, and ASEC follows this practice using either ASEC-BF cells or those supplied by customers.

2.0 CELL HOLDING FIXTURE

A variety of fixtures are used, depending on the size of the cell; if the cells are very fragile (thin or stressed slices) or the contacts are wraparound, a special fixture is used.

All these fixtures include a block which is controlled at preset temperatures by water pumped by a thermostatically controlled water bath, with feedback from a thermocouple embedded in the test block. These blocks also have vacuum hold-down facility and contain voltage and current probes for measurement of cell electrical output.

3.0 READOUT EQUIPMENT

The simulator has a digital meter, reading selected parameters V_{oc} , I_{sc} and the current at preset voltage levels. In addition, digital printout of these values, plus up to three other load voltage readings, are available.

Finally for development purposes, the I-V curves can be traced and from these, maximum, CFF and efficiency values can be estimated.

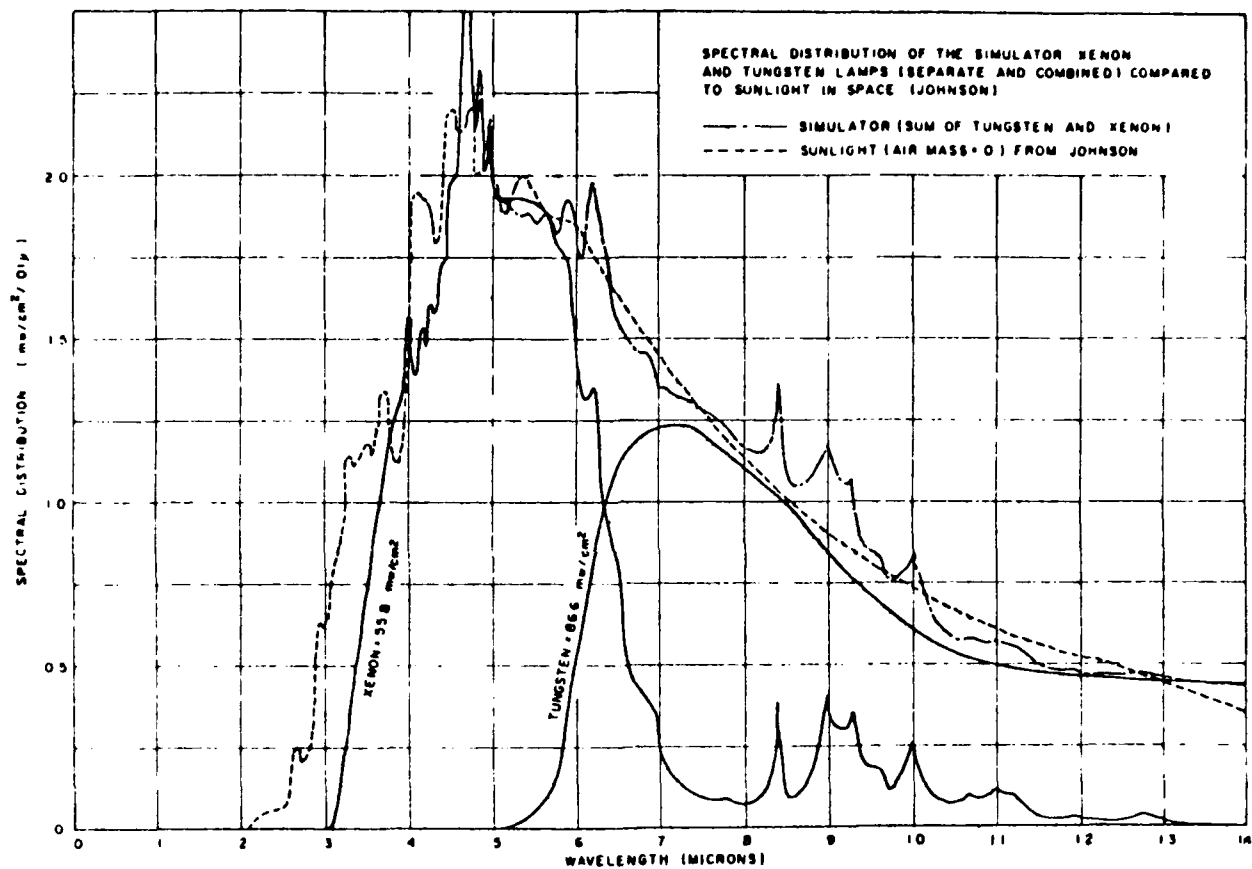


Figure A-1
 Spectral Distribution of the Simulator Xenon And
 Tungsten Lamps (Separate and Combined) Compared
 To Sunlight in Space (Johnson)

REFERENCES

- ¹ Solar Cell Array Design Handbook, Vol. 1, JPL, 1976, p. 4.5-1.
- ² Air Force Contract F33615-70-C-1619, Heliotek.
- ³ ESRO Contract 1407/71/AA, Electrical Research Association.
- ⁴ Air Force Contract F33615-67-C-1158, Ion Physics Corporation.
- ⁵ S. J. Marsk, et al, Conference Record of the 13th IEEE Photovoltaic Specialists Conference, 1978, pp. 624-627.
- ⁶ Air Force Contract F33615-70-C-1656, General Electric Company.
- ⁷ M. J. Rand and J. F. Roberts, J. Electrochemical Soc., Vol. 120, 1973, p. 446.
- ⁸ S. Zirinsky and E. A. Irene, J. Electrochem. Soc., Vol. 125, 1978, pp. 305-314.
- ⁹ Y. Koga, et al, Thin Film Dielectrics, Electrochem. Soc., 1969, pp. 335-377.
- ¹⁰ P. Iles, Applied Solar Energy Corporation, private communication.

BLANK PAGE

